

SEMMELWEIS EGYETEM
DOKTORI ISKOLA

Ph.D. értekezések

2971.

GREGOR ZSÓFIA

Szív-és érrendszeri betegségek élettana és klinikuma
című program

Programvezető: Dr. Merkely Béla, egyetemi tanár

Témavezető: Dr. Szűcs Andrea, egyetemi docens

**MORPHOLOGICAL AND FUNCTIONAL
INVESTIGATION AND DIFFERENTIAL
DIAGNOSTIC ASPECTS OF
HYPERTRABECULATION**

PhD Thesis

Zsófia Gregor MD

Doctoral School of Basic and Translational Medicine
Semmelweis University



Supervisor: Andrea Szűcs MD, Ph.D

Official reviewers: Róbert Pap MD, Ph.D

Zoltán Jambrik MD, Ph.D

Head of the Complex Examination Committee: István Karádi MD, D.Sc

Members of the Complex Examination Committee: Henriette Farkas MD, Ph.D

Hassan Charaf D.Sc

Budapest

2023

Table of Contents

List of abbreviations	5
1. Introduction	7
1.1. The structure and function of the normal myocardium	7
1.2. Ventricular trabeculation	7
1.2.1. The definition and embryogenesis of trabeculation	7
1.2.2. The role of trabeculation	8
1.2.3. The quantity of trabeculation.....	8
1.2.4. Trabeculation in the right ventricle	9
1.3. Ventricular trabeculation in physiological conditions.....	10
1.4. Ventricular trabeculation in pathological conditions.....	11
1.4.1. Extracardiac causes of ventricular hypertrabeculation.....	11
1.4.2. Cardiac causes of ventricular hypertrabeculation.....	12
1.4.3. Left ventricular noncompaction	13
1.4.4. Dilated cardiomyopathy	15
1.5. Imaging modalities in hypertrabeculation	16
1.5.1. Echocardiography.....	16
1.5.2. Magnetic resonance imaging	16
1.6. Questions and controversies about hypertrabeculation	19
2. Objectives	20
2.1. Sex- and age-specific normal values of left ventricular parameters using threshold-based trabecular quantification.....	20
2.2. MR-specific characteristics of left ventricular noncompaction and dilated cardiomyopathy	20
2.3. Characteristics of the right ventricle in left ventricular noncompaction with reduced ejection fraction	20
3. Methods	21

3.1. Study design and study populations	21
3.1.1. Study design and study population to determine sex- and age-specific normal values of left ventricular parameters through a threshold-based method	21
3.1.2. Study design and study population to examine the MR-specific characteristics of left ventricular noncompaction and dilated cardiomyopathy	23
3.1.3. Study design and study population to examine the characteristics of the right ventricle in left ventricular noncompaction with reduced ejection fraction	24
3.2. Image acquisition and analysis	26
3.3. Studied parameters	27
3.3.1. Studied parameters in the “Sex- and age-specific normal values of left ventricular parameters with a threshold-based method” study	27
3.3.2. Studied parameters in the “MR-specific characteristics of left ventricular noncompaction and dilated cardiomyopathy” study	27
3.3.3. Studied parameters in the “Characteristics of the right ventricle in left ventricular noncompaction with reduced ejection fraction” study	28
3.4. Statistical analysis	28
4. Results	30
4.1. Results of the “Sex- and age-specific normal values of left ventricular parameters with a threshold-based method” study	30
4.2. Results of the “MR-specific characteristics of left ventricular noncompaction and dilated cardiomyopathy” study	36
4.3. Results of the “Right ventricle in left ventricular noncompaction with reduced ejection fraction” study	45
The usage of contrast	45
5. Discussion	53
5.1. Discussion of the “Sex- and age-specific normal values of left ventricular parameters with a threshold-based method” study	53

5.2. Discussion of the “MR-specific characteristics of left ventricular noncompaction and dilated cardiomyopathy” study	56
5.3. Discussion of the “Right ventricle in left ventricular noncompaction with reduced ejection fraction” study.....	59
6. Limitations.....	62
7. Conclusion.....	63
8. Summary.....	65
9. References	66
10. Bibliography of the candidate’s publications	77
9.1. Publications related to dissertation	77
9.2. Publications not related to dissertation.....	77
10. Acknowledgement.....	79

List of abbreviations

ACM: arrhythmogenic cardiomyopathy

AHA: American Heart Association

ANOVA: analysis of variance

BMI: body mass index

BSA: body surface area

CI: confidence interval

CMR: cardiac magnetic resonance

CO: cardiac output

DCM: dilated cardiomyopathy

ECG: electrocardiogram

EDV: end-diastolic volume

EF: ejection fraction

ESC: European Society of Cardiology

ESV: end-systolic volume

FT: feature-tracking

FWS: free-wall strain

GCS: global circumferential strain

GLS: global longitudinal strain

HCM: hypertrophic cardiomyopathy

HT: subgroup with hypertrabeculated right ventricle

i: indexed values

ICC: intraclass correlation coefficient

IQR: interquartile range

LA: long-axis

LBBB: left bundle branch block

LGE: late gadolinium enhancement

LV: left ventricle

LVCM: left ventricular compacted myocardial mass

LVNC: left ventricular noncompaction

LVNC-N: left ventricular noncompaction with normal left ventricular function

LVNC-R: left ventricular noncompaction with reduced left ventricular function

MR: magnetic resonance

NT: subgroups with normal right ventricular trabeculation

RBR: rigid body rotation

RCM: restrictive cardiomyopathy

RV: right ventricle

SA: short-axis

SD: standard deviation

SD-TTP-CS: standard deviation of the time-to-peak circumferential strain

SD-TTP-LS: standard deviation of the time-to-peak longitudinal strain

SS: septal strain

SV: stroke volume

TB: threshold-based

TM: total myocardial mass

TPM: trabeculated and papillary muscle mass

1. Introduction

Trabeculae are part of the normal myocardial structure, but sometimes the trabeculation can be more extended than usual. Normal characteristics of trabeculae, possible diagnostic techniques, and differential diagnostic issues are presented in the following.

1.1. The structure and function of the normal myocardium

Histologically, the myocardium is a specific structure of individual striated muscles (1). The shortening of the heart muscle fibers enables the ejection of blood into the circulatory system during the systolic phase (1). Although cardiomyocytes compose a compact layer and form a functional unit, normally, there is a certain degree of trabeculation as a noncompact layer to support functional and structural tasks (2-4). The significant individual variability in trabeculation and the ratio of compacted-to-noncompacted layers raise further diagnostic and prognostic problems in cardiac imaging.

1.2. Ventricular trabeculation

1.2.1. The definition and embryogenesis of trabeculation

Trabeculae are defined as muscular columns projecting from the inner surface of the left (LV) and right ventricles (RV) of the heart or bundles of muscle connecting to other bundles of muscle in the ventricle's lumen (5). Trabeculae appear by the end of the 4th gestational week in humans and play a prominent role during embryogenesis: they increase the surface area and allow for an increase in myocardial mass in the absence of coronary circulation, and manage blood flow until the ventricles become functional (6). A recent study highlights the fundamental role of trabeculae in establishing the appropriate conduction pathway and conduction patterning in the developing ventricle (7).

Previous theories hypothesized that completed ventricular septation and increasing ventricular mass and volumes resulted in the compression of trabeculae within the chamber wall. Accordingly, the portion and thickness of the compact myocardium increase, while a thin layer remains from the noncompact layer, creating the structure of the developed myocardium (6). However, a recent review described that trabeculated layer reduction was never documented and there is no evidence for compaction in humans (8).

In contrast, the unequal proliferation of cardiomyocytes in the compact and trabeculated layers results in the normal structure of the myocardium (**Figure 1**) (9-11). As the proliferation is more intense in the compact layer and trabeculated layer grows slower, trabeculation is usually less prominent in the mature heart (12).

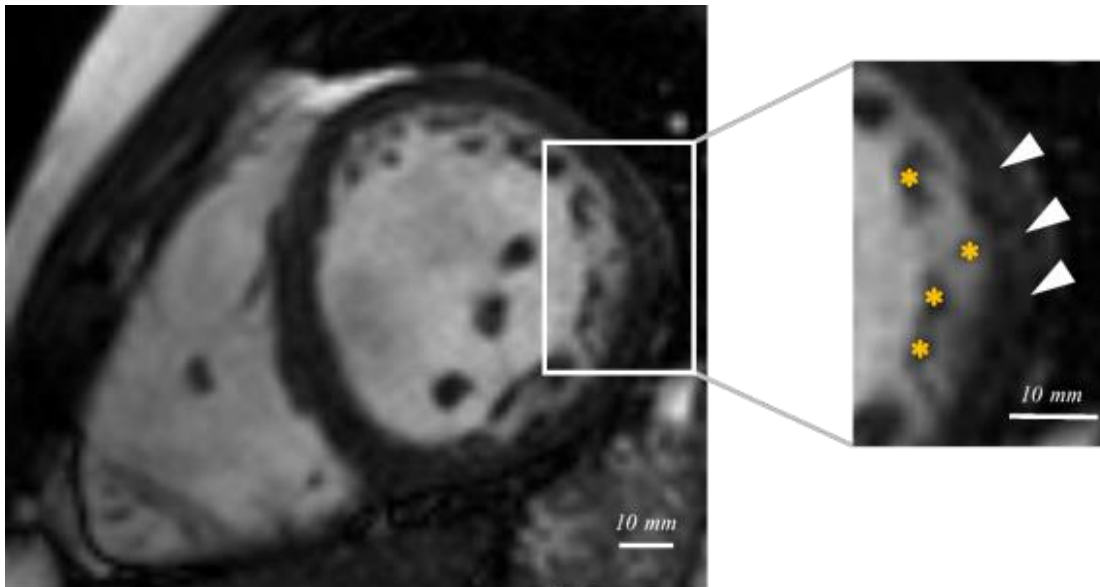


Figure 1 – CMR image from a healthy person with left ventricular hypertrabeculation (image of our working group). Yellow stars represent trabeculae in the left ventricle and white triangles represent the compacted myocardium on the enlarged image.

1.2.2. The role of trabeculation

Although trabeculae have numerous functions during embryogenesis, their role in the developed heart is not clearly defined. Presumably, besides the provided mechanical support, trabeculation contributes to the efficient filling and emptying of the chambers, moreover, it affects wall stress and diastolic compliance (3, 5, 13). The viscoelastic behavior of the trabeculae changes compared to that of the compact myocardial layers, and trabeculation affects the rate or magnitude of contraction and relaxation (14). Statical or functional problems might occur due to hypo- or hypertrabeculation.

1.2.3. The quantity of trabeculation

Hypo- and hypertrabeculation is not well defined since there is no uniform, globally accepted and used criterion for the normal amounts of trabeculae. For this reason, evaluation of trabeculation is sometimes challenging in cardiac imaging. As both hypo-

and hypertrabeculation may affect blood flow conditions and result in alteration of contractility, many studies have attempted to describe the normal values of trabeculae using different methods and techniques (15-21).

In animal experiments, hypotrabeculated mutants showed symptoms of heart failure and more frequent embryonic lethality (22). This indicates that trabeculation benefits cardiogenesis as part of normal cardiac structure and function. It also has a role in the development of normal conduction system (7, 23). Scarce human data are available regarding hypotrabeculation. Halaney et al. demonstrated on explanted human hearts and model simulations that loss in trabeculae resulted in decreased LV stiffness and increased LV compliance (5). Paun et al hypothesized that hypotrabeculation requires unnecessarily large strains with more energy which might result in reduced LV function (3).

In addition, LV hypertrabeculation can be observed in pathological conditions: left ventricular noncompaction (LVNC) is the most typical form, but excessive trabeculation can also occur in dilated cardiomyopathy (DCM) and other congenital diseases and cardiomyopathies (24-26). These entities will be explained in more detail thereafter.

1.2.4. Trabeculation in the right ventricle

Since the RV has specific characteristics with an individual geometry and a more expressed trabecular meshwork, the evaluation of RV hypertrabeculation is even more complex (**Figure 2**) (27, 28). The LV and RV are inseparable due to ventricular interdependency, as they are connected through mechanical interactions (27). As a result, RV involvement may be a consequence of the disease, but cardiomyopathies can also affect the RV itself (e.g. in arrhythmogenic cardiomyopathy (ACM), DCM or, presumably, LVNC) (29-32). Establishing the normal values of RV trabeculation could be helpful, as the RV in some pathological conditions (especially in cardiomyopathies) is still a preferred area of interest (33, 34).

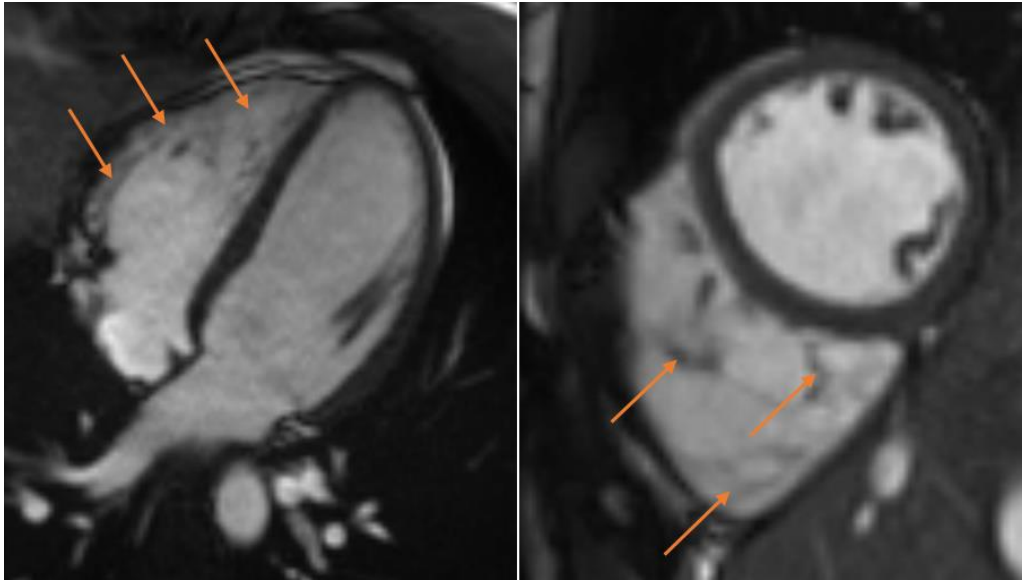


Figure 2 – Trabeculation in the right ventricle is represented with orange arrows on long-axis, four-chamber and short-axis CMR images from the same healthy person (images of our working group).

1.3. Ventricular trabeculation in physiological conditions

As mentioned above, trabeculae are part of the normal cardiac structure. Moreover, excessive LV trabeculation can be observed in 15-43% of the healthy population according to multiethnic studies conducted on large cohorts (2, 35). We also know that ethnicity and sex influence the quantity and complexity of trabeculation. African-Americans and Hispanic people have more trabeculae, while Chinese-Americans have less trabeculation compared to the white population (36). Furthermore, the thickness and amount of trabeculae are higher in males (2, 36).

Reversible LV hypertrabeculation can also be observed in some other physiological conditions with increased preload. Gati et al. found that increased preload might induce de novo LV trabeculation in 25% of pregnant women (37). Highly trained athletes also showed a higher prevalence of increased LV trabeculation, which was more pronounced in black athletes, suggesting the importance of genetic factors (38, 39). In these cases, the trabeculated ventricle can work at lower strains (which requires less energy) to maintain the same stroke volume (SV), than in a nontrabeculated ventricle, according to Paun et al. (3). **Figure 3** represents the different etiologies of LV hypertrabeculation.

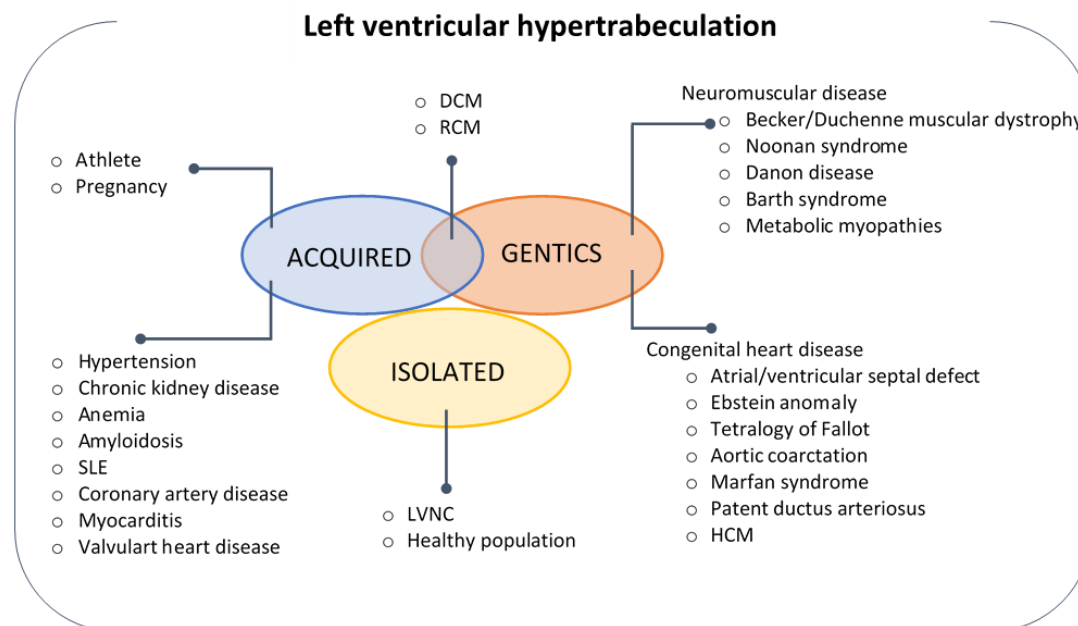


Figure 3 – Conditions with left ventricular hypertrabeculation (40).

(LVNC: left ventricular noncompaction; DCM: dilated cardiomyopathy; HCM: hypertrophic cardiomyopathy; RCM: restricted cardiomyopathy; SLE: systemic lupus erythematosus)

1.4. Ventricular trabeculation in pathological conditions

Extended LV trabeculation in pathological conditions might occur due to genetic factors or might be acquired, developmental or congenital (12, 40, 41). It can be associated with higher LV end-diastolic (EDV) and end-systolic volume (ESV) and lower ejection fraction (EF), according to a multi-ethnic study also (2, 42). In addition, ventricular trabeculation might occur with LV hypertrophy, or rarely, it can mimics restrictive cardiomyopathy (42). Trabeculae might become fibrotic in heart failure, decreasing LV compliance (5, 43). Nonetheless, a study with a 9.5-year follow-up described that LV trabeculation alone did not cause a decrease in LV function in healthy people (44).

1.4.1. Extracardiac causes of ventricular hypertrabeculation

There are also some extracardiac causes of LV hypertrabeculation, such as chronic kidney disease, sickle cell anemia, β -thalassemia and several neuromuscular disorders, for example Barth syndrome, Becker- or Duchenne muscular dystrophy (40, 45-50) (**Figure 3**).

1.4.2. Cardiac causes of ventricular hypertrabeculation

Cardiac causes of LV hypertrabeculation can be hypertensive heart disease, myocarditis, amyloidosis, and congenital heart disorders, such as Ebstein anomaly, tetralogy of Fallot, aortic coarctation, and patent ductus arteriosus (40, 51) (**Figure 3**). It is common in cardiomyopathies: DCM, hypertrophic cardiomyopathy (HCM), and rarely ACM or restrictive cardiomyopathy (RCM) can also be associated with LV hypertrabeculation (52, 53). Nonetheless, excessive LV trabeculation is most characteristic of LVNC. The differential diagnosis between these cardiomyopathies and conditions with LV hypertrabeculation, especially between LVNC and DCM, can be challenging, as they overlap genetically and morphologically (**Figure 4**) (54-56). Mutations in sarcomeric, cytoskeletal, Z-line, and mitochondrial proteins are responsible for genetic aspects (40, 57). Morphologically, the extended trabecular meshwork might cause a diagnostic challenge. The thinned compact myocardial layer, reduced LV function and dilated chambers complicates the evaluation process. It also raises the issue that it is not obvious whether hypertrabeculation is the cause or the consequence of the morphology in a given patient (40).

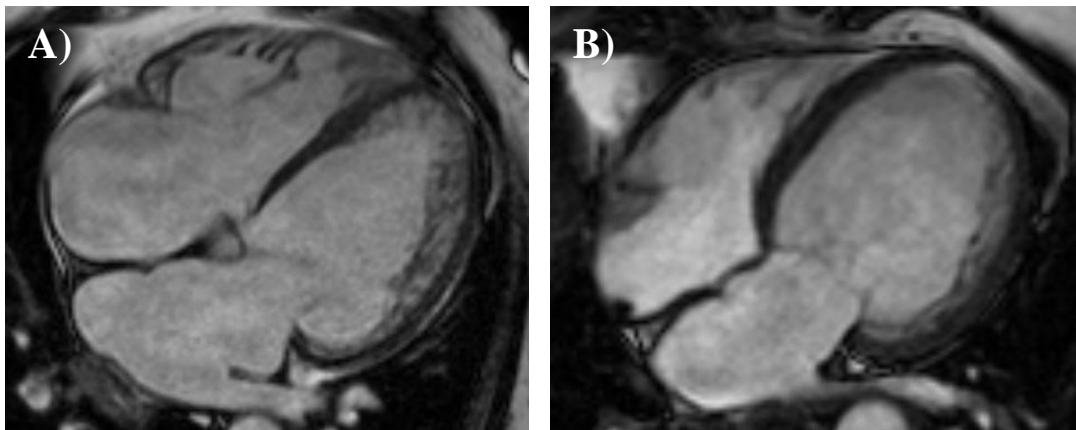


Figure 4 - The morphologically overlapping left ventricular noncompaction (A) and dilated cardiomyopathy (B); long-axis, four-chamber CMR images (images of our working group).

1.4.3. Left ventricular noncompaction

Excessive primary LV hypertrabeculation is a principal characteristic of LVNC morphology (55). Beside a thin, compact epicardial layer and a thicker trabeculated endocardial layer can be seen with deep intertrabecular recesses (55). Prominent LV trabeculation might associate with LV dilation and systolic dysfunction in some cases (58).

This morphology is classified as a primary genetic cardiomyopathy by the American Heart Association (AHA) and categorized as “other traits and syndromes associated with cardiomyopathy phenotypes” by the European Society of Cardiology (ESC) (58, 59).

The estimated prevalence of this condition in children and adults is between 0.02% and 0.14% (55, 60-62). Pathologically arrested compaction processes or altering proliferation of cardiomyocytes result in this entity (9-12).

In regard to the symptoms, a wide range of clinical manifestations is observable, from asymptomatic cases to thrombotic events, arrhythmias and heart failure (12, 62).

Compared to more widely available echocardiographic examinations, cardiac magnetic resonance imaging (CMR), with its better resolution and image quality, has become the gold standard for the examination of excessive trabeculation. The most frequently applied criteria for LVNC are proposed by Petersen et al., where the thickness ratio of noncompact-to-compact layers is >2.3 , and by Jacquier et al., where the trabeculated mass is more than 20% of the total myocardial mass (**Figure 5**) (15, 63). Other diagnostic criteria are based on the fractal dimension or the portion or ratio of trabeculation (64-66). As diagnostic criteria based on only morphological features do not well distinguish the benign form of excessive trabeculation from noncompact cardiomyopathy and many patients are overdiagnosed, an integrated diagnostic approach was suggested by Vergani et al. (67). In this risk stratification model, the patient’s clinical history, family history, electrocardiogram (ECG) and Holter monitoring results, genetic tests, and presence of late gadolinium enhancement (LGE) on CMR images are also part of the diagnostic algorithm (67). Accordingly, patients with noncompaction phenotype and normal EF do not require further follow-up (67, 68). This proceeding is also suggested by a state-of-the-art review from Petersen et al. (12). However, left ventricular dysfunction and LGE are the principal indicative factors for adverse outcomes in cases of excessive LV trabeculation (69, 70). RV size and function might also be prognostic markers,

highlighting the importance of RV involvement in LVNC (71). Nonetheless, subjects with normal LV function and without any of the abovementioned red flags do not need further assessment (67).

We would like to highlight the RV, whose involvement in noncompaction is controversial and still the subject of many investigations (34, 72, 73). Since neither the normal value of RV trabeculation nor the involvement of the RV is well known, our research group has performed large cohort studies on noncompacted patients with good EF to answer these questions (33, 34). Another important question is how the noncompaction of LV and the deterioration of LV function influence the RV in this condition.

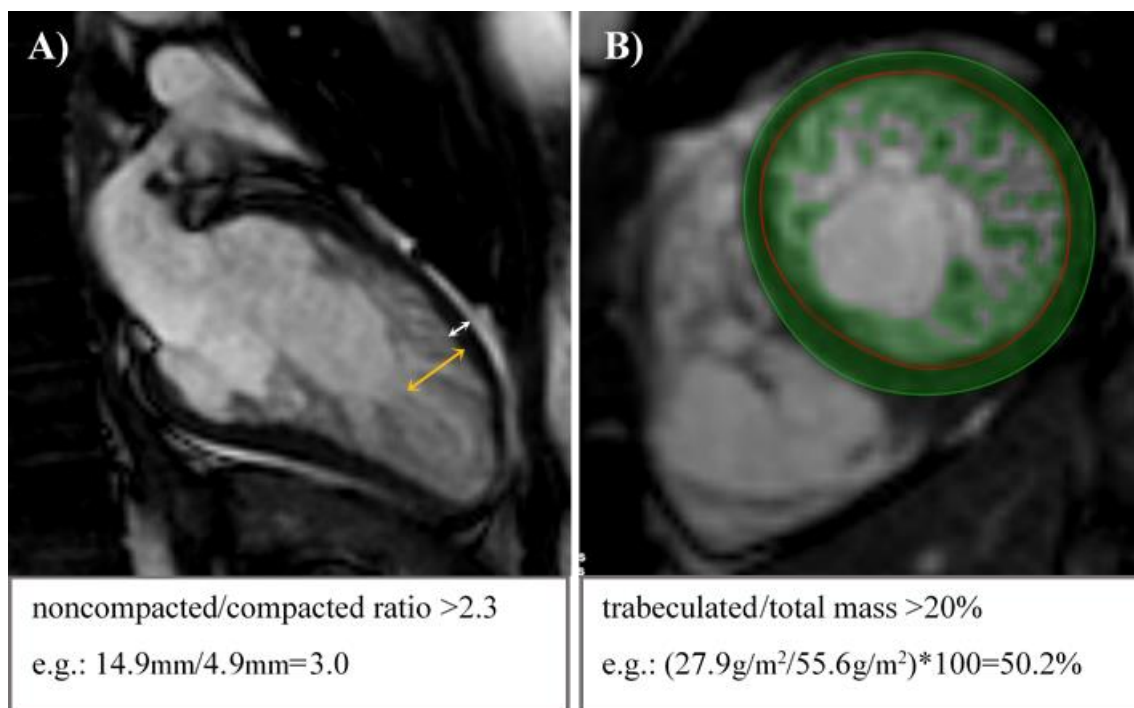


Figure 5 – CMR images represent the diagnostic criteria of left ventricular noncompaction. Image (A) showing the diagnostic criterion of Petersen: the yellow arrow represents the noncompacted layer, while the white arrow represents the compact layer in long-axis scan, end-diastole. Image (B) represents the diagnostic criterion of Jacquier: trabeculae are seen with green within the red endocardial contour (images of our working group).

1.4.4. Dilated cardiomyopathy

DCM is characterized by enlargement and dysfunction of the LV in the absence of abnormal loading conditions (e.g. hypertension or valve disease) or coronary artery disease (74). Due to cardiac remodeling, the atriums and RV might also be affected besides the LV, which predicts a worse prognosis (31, 75). The estimated prevalence of the disease is around 1:2500, from which 30-50% are counted as primary DCM with genetic background (59). In addition to primary DCM, secondary DCM can occur due to infectious agents, drugs and toxins, endocrine, autoimmune, and neuromuscular disorders, or rarely pregnancy (named peripartum cardiomyopathy) (59, 74).

Patients with DCM may develop symptoms of heart failure (e.g. dyspnea, palpitation, peripheral edema), arrhythmias, thromboembolic events or even sudden cardiac death might also occur (54).

Echocardiography has its role in the diagnosis, but the gold standard is CMR, which, in addition to the precise evaluation of morphological and functional parameters, has additional value in determining the etiology using LGE and tissue characterization (T1, T2 mapping) (54).

Pharmacological treatment of the symptoms (mostly heart failure), or if it is insufficient, device therapy (implantable cardioverter-defibrillator, cardiac resynchronization therapy or mechanical circulatory support) may be applicable if indicated (76). Despite the wide range of therapeutic options, DCM is the most frequent cause of heart transplantation (59).

We must highlight that volume overload might induce LV hypertrabeculation in some patients, causing differential diagnostic problems from LVNC. Despite comparable morphology and therapy, the clinical importance of accurate diagnosis could aid in risk stratification, indicating the need for early initiation of anticoagulant therapy or early family screening, even for asymptomatic patients with hypertrabeculation (67, 77).

1.5. Imaging modalities in hypertrabeculation

1.5.1. Echocardiography

As transthoracic echocardiography is widely available, it is the first examination method of cardiac hypertrabeculation in most cases. Several investigations have described potential diagnostic criteria of LVNC using echocardiography, but poor agreement has been observed between them (78-81). Contrast echocardiography can provide incremental data to non-contrast echocardiography, as delineation of trabeculae might allow additional diagnostic opportunities (82). Deformation analysis of the myocardium can also be done through speckle-tracking echocardiography, which can be helpful in the early diagnosis or risk stratification of LVNC, while rotation analysis might also have additional diagnostic value for hypertrabeculation (83-86). Nonetheless, echocardiography is usually used for the assessment of LV function and follow-up of patients with hypertrabeculation in everyday practice.

1.5.2. Magnetic resonance imaging

Compared to echocardiography, CMR enables more objective imaging with high reproducibility. Thanks to its greater resolution and reliable blood-myocardial differentiation with better visualization of trabeculae, CMR has become the gold standard for characterizing myocardial structural disorders (12).

A position statement suggested the inclusion of trabeculae principally in the myocardial mass if possible, and otherwise in blood volume (87). Nevertheless, in general practice, trabeculae are added to volumetric parameters, and only the presence of hypertrabeculation indicates the quantification of trabecular mass separately. The isolation of trabeculae would be necessary in these cases, as it might have clinical relevance. Several methods of measuring trabeculae are known, and as manual contouring of trabeculae is less precise and has high interobserver variability, we used a more objective and accurate method in our investigations. The applied threshold-based (TB) technique is based on the differing signal intensities of blood and myocardium. After the manual correction of semiautomatically traced epi- and endocardial contours in end-diastole and end-systole, the program identifies each voxel as blood or myocardium according to the threshold setting. Thus, the epicardial contours include the total myocardial mass (TM), and within the endocardial borders, the trabeculated and papillary

muscle mass (TPM) value is precisely measurable (**Figure 6**). Although this method does not differentiate trabecular from papillary muscles, their segmentation is not crucial in clinical practice (21). In contrast to conventional contouring techniques (i.e., manual contouring), the TB method is highly reproducible and independent of the experience of the observer (88-90). However, as TPM is calculated as a separate parameter, the volumetric, myocardial mass, and EF values differ significantly from those calculated with the traditional method (18, 91). These differences in the measured parameters might have clinical relevance.

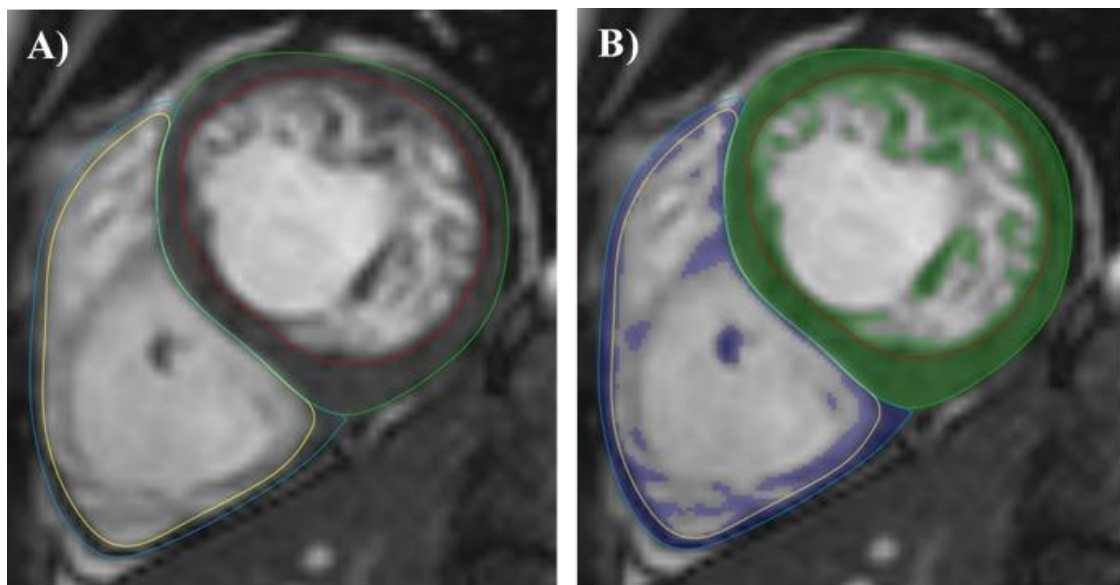


Figure 6 – Representative images of the contouring techniques.

Image (A) represents conventional, manually corrected semiautomatic contours, and image (B) represents the threshold-based algorithm. Epicardial contours are marked with green or blue lines, while endocardial contours are marked with red or yellow lines in the left ventricle or right ventricle, respectively. In image (B), green and blue areas represent the total detected left or right ventricular myocardial mass within the epicardial contours, while trabecular mass is calculated within the endocardial contours. The grey area corresponds to blood volumes in the cavity of the ventricles and in the intertrabecular recesses as well (images of our working group).

A further postprocessing evaluation possibility is the feature-tracking (FT) technique used for deformation analysis and assessing regional myocardial function (**Figure 7**) (92). Myocardial strain measures the percent change in myocardial length from relaxed to

contracted status by tracking identified features in subsequent frames throughout the cardiac cycle (92, 93). Strains can be calculated globally or segmentally in longitudinal, circumferential, and radial directions. We need to mention that calling the strains lower or higher (i.e., worse and better) is based on the changes in their absolute values. In addition, the prognostic role of the strains in adverse cardiac outcomes should be highlighted (93).

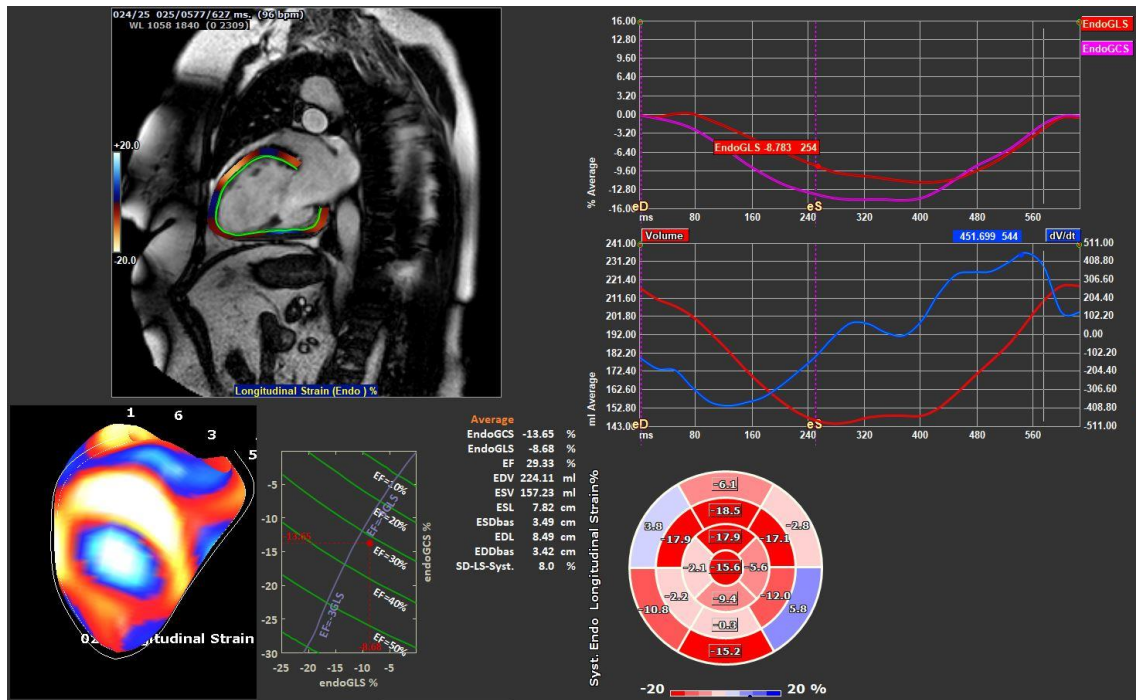


Figure 7 – Representative image of feature-tracking strain analysis from the QMass module of Medis Suite software (Version 3.2, Medis Medical Imaging Systems, Leiden, the Netherlands)

The standard deviations of the time-to-peak strain values were calculated to estimate the intraventricular synchronous contraction and the mechanical dispersion in longitudinal and circumferential directions.

Strain values are also suitable for rotational pattern analysis. The systolic peak rotations of the apical and basal parts can be described, which normally have a clockwise direction in the basal segments (negative value) and counterclockwise in the apical parts (positive value) (94, 95). Regarding rotational directions, we distinguished normal rotation (-/+), reverse rotation (+/-), and positive (+/+) or negative (-/-) rigid body rotation (RBR).

We also have to mention LGE, which is based on connective tissue remodeling and common in cardiomyopathies. Besides the ischemic origin, inflammatory and immune processes could also mediate fibrosis (96). The pattern of the myocardial fibrosis-caused hyperenhanced signal in the expanded extracellular spaces is characteristic of different cardiomyopathies. The disease and also comorbidities might be the cause of LGE, and the prognostic role of LGE in clinical practice should also be emphasized.

1.6. Questions and controversies about hypertrabeculation

Although several studies have focused on noncompaction in the last decade, its evaluation and classification are controversial. The different categorization of AHA and ESC, and the changes in the latest ESC guideline regarding the classification of LVNC suggest that we still have a lot to know about this entity (12, 58, 59).

There is no consensus on the general, uniformly applied measurement of trabeculae in cardiac imaging. However, the differentiation of normal and excessive trabeculation would be necessary for adequate patient follow-up (97). Trabecular quantification with objective post-processing CMR techniques might be helpful in this question. Differential diagnostic issues might also occur in physiological hypertrabeculation and cardiomyopathies. Nonetheless, the evaluation of hypertrabeculation with reduced LV function is challenging: extended trabeculation can be the consequence or even the cause of decreased pump function (3). Moreover, decreased LV function might also effect RV parameters. The involvement of RV in noncompaction and the connections between RV and LV parameters are still not well known, and require further investigations (32).

2. Objectives

Our research aimed to describe sex- and age-specific normal values of the LV using the TB method and to study ventricular hypertrabeculation in different cardiac conditions in both the LV and RV.

2.1. Sex- and age-specific normal values of left ventricular parameters using threshold-based trabecular quantification

The undefined border between normal and excessive trabeculation and the lack of normal values of the trabecular mass determined using the TB method point out the need to describe new reference ranges for LV parameters using this technique, which calculates cardiac volumes and myocardial mass parameters differently from the conventional mode. We aimed to define sex- and age-related normal reference ranges for LV volumetric, functional, and myocardial mass values and the correspondences and temporal changes of these parameters with the TB method.

2.2. MR-specific characteristics of left ventricular noncompaction and dilated cardiomyopathy

As DCM and LVNC with reduced LV-EF could be genetically and morphologically overlapping conditions, the differential diagnostic issues by CMR may be challenging. Our purpose was to investigate the differences and similarities in the LV volumetric, functional, and myocardial mass parameters and strain values between patients with LVNC and reduced LV-EF and patients with nonischemic DCM.

2.3. Characteristics of the right ventricle in left ventricular noncompaction with reduced ejection fraction

The LV and RV are inseparable through mechanical interactions, but RV characteristics in the case of hypertrabeculated LV and the effect of LV function deterioration on RV parameters in LVNC are less well described.

Thus, we aimed to investigate the characteristics of the RV and quantify the connections between RV parameters, LV function, and trabeculation in LVNC patients with reduced LV function (LVNC-R). We compared these correspondences with those in DCM patients and LVNC subjects with normal LV function (LVNC-N).

3. Methods

3.1. Study design and study populations

3.1.1. Study design and study population to determine sex- and age-specific normal values of left ventricular parameters through a threshold-based method

This investigation was a single-center study with 200 healthy European adults. The enrolled volunteers completed a questionnaire about demographic details, medical history, medication, cardiovascular symptoms, and sport activity. In addition to CMR examinations, blood pressure measurements and 12-lead resting ECG were performed for each participant. The study population was divided by age with an equal number of male and female participants in each group: 20–29 years (Group A, n = 50), 30–39 years (Group B, n = 50), 40–49 years (Group C, n = 50) and ≥ 50 years (Group D, n = 50).

We applied the following exclusion criteria: congenital cardiac abnormalities or acquired ischemic heart diseases, arrhythmias, valvular heart diseases, cardiomyopathies, other cardiac disorders, and sudden cardiac death in the family history. Participants with extracardiac diseases, including hypertension-related, pulmonary, nephrology, gastrointestinal, metabolic, autoimmune, hormonal, psychiatric, oncologic, neuromuscular disorders, or other hereditary conditions, were also excluded. None of the participants had received medical therapy. Athletes who engaged in competitive sport activity (>6 hours/week) were also excluded (98). The baseline characteristics are presented in **Table 1**.

All procedures in this study were in accordance with the 1964 Helsinki Declaration and its later amendments or comparable ethical standards. Ethical approval was obtained from the Semmelweis University Regional and Institutional Committee of Science and Research Ethics, and all participants provided written informed consent (165/2017).

Table 1 - Baseline characteristics of the total healthy population and its subgroups: Group A: 20-29 years; Group B: 30-39 years; Group C: 40-49 years; Group D: ≥ 50 years. Values are presented as mean \pm SD.

(BMI: body mass index, BSA: body surface area)

		Age (years)	BMI (kg/m²)	BSA (m²)
Total population (n=200)	Total	39.4 \pm 12.0	24.3 \pm 3.6	1.9 \pm 0.2
	Male (n=100)	39.6 \pm 12.3	25.8 \pm 3.1	2.1 \pm 0.2
	Female (n=100)	39.2 \pm 11.8	22.8 \pm 3.3	1.7 \pm 0.1
	p	0.82	<0.0001	<0.0001
Group A (n=50)	Male (n=25)	24.5 \pm 3.2	24.2 \pm 3.4	2.0 \pm 0.1
	Female (n=25)	24.1 \pm 3.2	21.1 \pm 2.9	1.7 \pm 0.1
	p	0.66	0.0012	<0.0001
Group B (n=50)	Male (n=25)	33.6 \pm 2.6	26.4 \pm 2.8	2.1 \pm 0.2
	Female (n=25)	33.6 \pm 2.7	22.6 \pm 4.1	1.7 \pm 0.2
	p	0.96	0.0004	<0.0001
Group C (n=50)	Male (n=25)	44.8 \pm 3.1	26.4 \pm 3.0	2.1 \pm 0.2
	Female (n=25)	44.8 \pm 2.3	22.7 \pm 2.5	1.7 \pm 0.1
	p	0.92	<0.0001	<0.0001
Group D (n=50)	Male (n=25)	55.7 \pm 4.3	26.4 \pm 2.8	2.1 \pm 0.1
	Female (n=25)	54.4 \pm 3.4	24.6 \pm 2.8	1.8 \pm 0.1
	p	0.25	0.03	<0.0001

3.1.2. Study design and study population to examine the MR-specific characteristics of left ventricular noncompaction and dilated cardiomyopathy

In this retrospective study, we enrolled 31 nonischemic DCM patients, 42 LVNC patients, and 42 healthy controls.

In the DCM population, the following diagnostic criteria were applied: 1) dilated LV chamber with increased LV volume (LV-EDVi males: $>112\text{ml/m}^2$, females: $>99\text{ml/m}^2$), 2) impaired systolic LV function (EF $< 50\%$), and 3) the exclusion of other causes of LV dysfunction (74, 99).

The diagnosis of LVNC was made if we saw 1) a bilayered LV wall structure of noncompacted and compacted myocardium; 2) a prominent trabecular meshwork that fulfilled of the criterion of Petersen, namely, the ratio of the thicknesses of the noncompact and compact myocardial layers was greater than 2.3 in end-diastole; 3) the fulfillment of the Jacquier criterion, namely, the value of trabeculated LV mass was more than 20% of the total myocardial mass. In addition, decreased systolic LV function (EF $<50\%$) was an enrollment criterion (15, 63).

The patient groups were matched by sex and age with a healthy control population without any comorbidities.

The following exclusion criteria were applied for all groups: coronary artery diseases, valvular or congenital heart disorders or other cardiomyopathies, and any relevant comorbidities, e.g., hypertension or diabetes mellitus. The presence of implanted devices (e.g., implantable cardioverter defibrillator) or pacemakers was also an exclusion criterion. SA cine images performed after contrast agent administration or images containing arrhythmic or respiratory artifacts were also ruled out. The main characteristics of the populations are listed in **Table 2**.

Ethical approval was obtained from the Semmelweis University Regional and Institutional Committee of Science and Research Ethics, and all participants provided informed consent (OGYÉI/7397/2019).

Table 2 – Baseline characteristics of the dilated cardiomyopathy, left ventricular noncompaction, and control groups. Values are presented as mean \pm SD or n (%).

(DCM: dilated cardiomyopathy; LVNC: left ventricular noncompaction; C: controls; BSA: body surface area)

	DCM (n=31)	LVNC (n=42)	CONTROL (n=42)	P (DCM vs. LVNC)	P (DCM vs. C)	P (LVNC vs. C)
Sex category (men) n (%)	18 (58)	30 (71)	30 (71)	0.45	0.45	1
Age (year)	51.3 \pm 14.8	55.2 \pm 11.2	52.9 \pm 8.1	0.31	0.82	0.61
BSA (m ²)	1.99 \pm 0.2	1.96 \pm 0.3	1.97 \pm 0.2	0.77	0.90	0.96

3.1.3. Study design and study population to examine the characteristics of the right ventricle in left ventricular noncompaction with reduced ejection fraction

We retrospectively included 44 LVNC-R patients (EF<50%), 44 LVNC-N participants (EF \geq 50%), and 31 DCM patients in this investigation.

The diagnosis of LVNC was based on the morphological criterion of Petersen, and we also applied the Jacquier criterion for better patient selection (15, 63). In addition to these morphological criteria, at least one clinical symptom had to be reported in the anamnestic details of the LVNC participants, as recommended by Vergani et al. (**Table 12**) (67).

DCM patients had the following diagnostic criteria: dilated LV chamber with increased LV volumes (LV-EDVi males: >112ml/m², females: >99 ml/m²), and decreased systolic LV function (EF<50%), with the exclusion of other causes of LV dysfunction (74, 99).

The exclusion criteria were the following: ischemic, valvular, or congenital heart diseases or other coexisting cardiomyopathy; another relevant comorbidity (hypertension, diabetes mellitus, endocrine disorders, chronic kidney or systemic diseases, etc.); or intense sports activity (>6 hours/week). Patients whose image quality was poor, whose scans were performed after contrast agent administration, or whose images showed arrhythmic or respiratory artifacts were also excluded (100). The main characteristics of the groups are given in **Table 3**.

To investigate RV hypertrabeculation in more detail, the groups were divided into two subgroups by the amount of RV trabeculation. For this, we applied the sex- and age-specific reference ranges for RV trabeculated mass established by our research team in another, large CMR study with a similar postprocessing technique (33). All participants were evaluated individually by age and sex based on these normal ranges. Those who exceeded that range were classified as participants with RV hypertrabeculation (HT), while those who were within the abovementioned reference range were classified as having normal RV trabeculation (NT).

All procedures in this investigation followed the 1964 Declaration of Helsinki and its later amendments or comparable ethical standards. Ethical approval was obtained from the Central Ethics Committee of Hungary (OGYÉI/7397/2019). All participants provided written informed consent.

Table 3 - Baseline characteristics of the studied dilated cardiomyopathy and left ventricular noncompaction populations. Values are presented as mean \pm SD or n (%). (DCM: dilated cardiomyopathy; LVNC-R: left ventricular noncompaction with reduced left ventricular function; LVNC-N: left ventricular noncompaction with good left ventricular function; BSA: body surface area; BMI: body mass index)

	DCM (n=31)	LVNC-R (n=44)	LVNC-N (n=44)	p (LVNC-R vs.DCM)	p (LVNC-R vs.LVNC-N)	p (DCM vs.LVNC-N)
Sex category (man) n (%)	18 (58)	30 (68)	30 (68)	0.37	1	0.37
Age (years)	51.3 \pm 14.8	55.4 \pm 11.0	45.8 \pm 13.3	0.36	0.002	0.17
BSA (m ²)	1.99 \pm 0.23	1.96 \pm 0.26	1.98 \pm 0.22	0.86	0.93	0.98
BMI (kg/m ²)	27.7 \pm 5.1	26.5 \pm 5.5	26.3 \pm 3.7	0.52	0.99	0.45

3.2. Image acquisition and analysis

CMR examinations were performed on 1.5 T scanners (Magnetom Aera, Siemens Healthineers, Erlangen, Germany; or Achieva, Philips Medical System, Eindhoven, the Netherlands).

Retrospectively gated, balanced steady-state free-precession cine images were acquired in conventional 2-, 3- and 4-chamber long-axis (LA) views. Breath-hold short-axis (SA) cine images from base to apex were obtained with full coverage of the LV and RV.

The scanning parameters were the following for the respective scanners: repetition time: 2.5 and 2.7 ms; echo time: 1.15 and 1.3 ms; flip angle: 58° and 60°; spatial resolution: 1.5 × 1.5 mm for both scanners; and temporal resolution: 25 frames per cardiac cycle for both scanners. The slice thickness was 8 mm with no interslice gap, and the field of view was 350 mm on average, adapted to body size.

Gadolinium-based contrast agent gadobutrol (Gadovist, Bayer-Schering, 0.15 ml/kg) was administered when it was required for the accurate diagnosis and the patient gave written consent. It was not given to healthy control participants. To optimize the image quality, the images were obtained before the administration of the contrast agent (100). In the “MR-specific characteristics of left ventricular noncompaction and dilated cardiomyopathy” study, LGE was evaluated segmentally in all patients.

For the postprocessing analysis, Medis Suite software (Version 3.2, Medis Medical Imaging Systems, Leiden, the Netherlands) and its QMass and QStrain modules were used. After identification of the end-systolic and end-diastolic phases of the cardiac cycle, semiautomatic tracing and manual correction of the endo- and epicardial contours of the LV and RV were performed from the base to the apex. The contours were made by two independent observers with 5 and 11 years of experience for each material.

All of the measured LV and RV parameters were calculated by the TB method using the MassK algorithm and the QMass module of Medis Suite software. The algorithm calculates a blood fraction value in all given voxels based on their signal intensity (90). Thresholding this value, voxels above the applied threshold are considered pure blood, and voxels below this threshold are considered pure muscle (90). The threshold was set to the default (50%) recommended by the Medis Medical System and was not modified during the postprocessing analysis.

The FT strain analysis within the QStrain module of Medis Suite software was used for the LV and RV deformation analysis. In our studies, subendocardial strain values were calculated based on the traced endocardial borders in the SA, the 2-, 3- and 4-chamber LA images of the LV, and the 4-chamber view of the RV. Global and segmental strains were measured in both ventricles. To avoid possible inaccuracies of the segmental strain measurement, the average values of the apical, middle, and basal segments were calculated based on the 16- and 17-segment models in the LV (101).

End-diastolic SA scans were used to measure LV wall thicknesses, according to the 16-segment model (101).

3.3. Studied parameters

3.3.1. Studied parameters in the “Sex- and age-specific normal values of left ventricular parameters with a threshold-based method” study

The following LV parameters were calculated with the TB method: EDV, ESV, SV, cardiac output (CO), EF, end-diastolic TM, and end-diastolic TPM. As the program does not determine the LV compact myocardial mass (CM) values directly, we calculated it as the difference between LV-TM and LV-TPM. We used only LV-CM and LV-TPM to characterize the myocardium in this study. All measured parameters were indexed (i) to body surface area (BSA). Different ratios were created for the assessment of the correspondences of LV parameters: trabeculated and papillary muscle mass-to-compact myocardial mass (LV-TPMi/LV-CMi) ratio, the compact myocardial mass-to-end-diastolic volume (LV-CMi/LV-EDVi) ratio, and the trabeculated and papillary muscle mass-to-end-diastolic volume (LV-TPMi/LV-EDVi) ratio.

3.3.2. Studied parameters in the “MR-specific characteristics of left ventricular noncompaction and dilated cardiomyopathy” study

We also used the TB method in this investigation to calculate the following LV parameters: EDV, ESV, SV, EF, TPM, and CM, indexed to BSA.

The FT technique was used for the deformation analysis, where LV global longitudinal (LV-GLS) and global circumferential strain (LV-GCS) values were established, and segmental strains were calculated as the average values of the apical, middle, and basal segments.

The mechanical dispersion was estimated as the standard deviation of the time-to-peak strain values in the longitudinal (SD-TTP-LS) and circumferential directions (SD-TTP-CS).

In the following, the abovementioned rotational patterns were observed in the groups: normal rotation (-/+), reverse rotation (+/-), and positive (+/+) or negative (-/-) RBR.

Based on the CMR images and reports, left bundle branch block (LBBB) was also investigated in the patient groups.

In addition to the abovementioned parameters, LGE and wall thickness were identified.

3.3.3. Studied parameters in the “Characteristics of the right ventricle in left ventricular noncompaction with reduced ejection fraction” study

The following parameters were calculated in both the LV and RV using the TB method: EDV, ESV, SV, EF, TM and TPM. The compact myocardial mass of both ventricles was determined as mentioned above. All parameters were indexed to BSA.

We also used strain measurements for the deformation analysis with the FT technique. The global function of the ventricles was evaluated with LV-GLS, LV-GCS, and RV-GLS values, and RV free-wall strain (FWS) and RV septal strain (SS) were calculated to describe segmental RV function.

3.4. Statistical analysis

The normality of variable distributions was assessed with the Kolmogorov–Smirnov test or the Shapiro–Wilk test. Continuous variables are reported either as the mean \pm standard deviation (SD) or as the median [interquartile range] (IQR) as appropriate. Categorical variables are expressed as counts and percentages. The 95% confidence intervals (CIs) were calculated to assess the normal ranges for LV parameters.

In comparing two groups, the independent-sample t-test was applied to compare parameters that fit a normal distribution; otherwise, the Mann–Whitney test was used.

ANOVA with Tukey's post hoc test was used to compare the three groups in the case of normal distribution and equal variances, while non-normally distributed data were compared by the Kruskal–Wallis test with Dunn's test. The chi-squared test was performed to compare categorical variables.

Pearson's or Spearman's correlation coefficient was calculated to assess the linear correlations between the studied parameters.

The intraclass correlation coefficients (ICCs) were calculated to determine the interobserver variability and reported with 95% confident interval (interpreted as: 0.4-0.75 - fair to good, greater than 0.75 - excellent). We considered a p value <0.05 statistically significant.

The statistical analysis was performed using MedCalc Statistical Software (Version 17.9.5, MedCalc Software, Ostend, Belgium) or the IBM SPSS Statistics (Version 25.0, IBM Corp., Armonk, New York, USA).

4. Results

4.1. Results of the “Sex- and age-specific normal values of left ventricular parameters with a threshold-based method” study

Interobserver variability

Interobserver variability was determined by the global ICC, which represents all of the measured LV parameters' interobserver agreements. It was tested on 20 (10%) randomly selected participants and calculated at 0.92 (0.82-0.98), indicating excellent interobserver variability.

Sex- and age-specific normal values of LV parameters

Mean \pm SD or median [IQR], and the 95% CIs of LV volumetric and functional parameters, myocardial mass values, and derived parameters were assessed in the total study population and in each age group divided by sex (**Table 4 A and B**). LV-EDVi, LV-ESVi, LV-EF, LV-CMi, and LV-TPMi differed significantly between males and females in the total population. The volumetric and myocardial mass parameters were higher, while the LV-EF was lower in males compared to females (**Table 4 A and B**). Dividing the participants by age and sex, unlike the volumetric and functional parameters, the LV-CMi and LV-TPMi values differed significantly in all age groups. However, the difference in the LV-TPMi/LV-CMi ratio remained nonsignificant between the sexes. The LV-CMi/LV-EDVi and LV-TPMi/LV-EDVi ratios also showed significant differences between males and females in most of the age groups (**Table 4B**).

Table 4 - Description of age- and sex-related left ventricular (LV) parameters (102). Values are presented as mean \pm SD for normally distributed data or median with [IQR] for non-normally distributed data. 95% CI was also calculated. ANOVA and Tukey post hoc test or Kruskal-Wallis tests and Dunn post hoc test was used, as appropriate. \square $p < 0.05$ vs Group A; & $p < 0.05$ vs Group B; \$ $p < 0.05$ vs Group C; # $p < 0.05$ vs Group D (LV-EDVi: LV end-diastolic volume index; LV-ESVi: LV end-systolic volume index; LV-SVi: LV stroke volume index; LV-COi: LV cardiac output index; LV-EF: LV ejection fraction; LV-CMi: LV end-diastolic compacted myocardial mass index; LV-TPMi: LV end-diastolic papillary and trabeculated muscle mass index; SD: standard deviation; CI: confidence interval)

A)	Group		Male	Female	p (sex)
LV-EDVi (ml/m ²)	Total	Mean±SD	69.5 ± 10.7	64.5 ± 8.5	0.0003
		95% CI	51.8 - 93.8	50.0 - 82.2	
	A	Mean±SD	73.2 ± 11.5 [#]	68.3 ± 10.4 [#]	0.12
		95% CI	54.5 - 96.9	53.9 - 97.2	
	B	Mean±SD	68.6 ± 10.4	64.7 ± 6.1	0.11
		95% CI	48.7 - 93.2	53.0 - 77.6	
	C	Mean±SD	71.4 ± 9.5	66.0 ± 7.5 [#]	0.03
95% CI		53.8 - 91.3	51.5 - 81.5		
D	Mean±SD	64.6 ± 10.1 [□]	58.9 ± 6.8 [□] [§]	0.02	
	95% CI	51.8 - 87.0	48.0 - 71.6		
p (age)			0.03	0.001	
LV-ESVi (ml/m ²)	Total	Mean±SD	22.7 ± 5.2	19.3 ± 4.1	<0.0001
		95% CI	13.7 - 33.6	12.3 - 29.7	
	A	Mean±SD	25.1 ± 5.3 [#]	20.7 ± 4.1 [#]	0.002
		95% CI	17.1 - 36.0	14.9 - 30.0	
	B	Mean±SD	22.6 ± 4.7	19.9 ± 3.7 [#]	0.03
		95% CI	13.7 - 32.4	13.8 - 27.8	
	C	Mean±SD	22.2 ± 4.9	19.7 ± 4.5 [#]	0.07
95% CI		14.0 - 33.6	12.1 - 29.5		
D	Mean±SD	21.1 ± 5.4 [□]	16.8 ± 3.0 [□] & [§]	0.001	
	95% CI	12.2 - 33.0	12.0 - 22.4		
p (age)			0.04	0.003	
LV-SVi (ml/m ²)	Total	Mean±SD	46.6 ± 7.8	45.1 ± 6.1	0.13
		95% CI	34.1 - 61.7	34.4 - 57.9	
	A	Mean±SD	48.0 ± 8.3	47.4 ± 7.1 [#]	0.77
		95% CI	34.9 - 66.7	38.1 - 65.9	
	B	Mean±SD	46.1 ± 7.1	44.7 ± 3.9	0.41
		95% CI	34.4 - 61.0	38.1 - 52.6	
	C	Mean±SD	48.8 ± 6.7	46.3 ± 5.7	0.16
95% CI		34.6 - 59.7	35.5 - 56.4		
D	Mean±SD	43.6 ± 8.2	42.1 ± 6.3 [□]	0.49	
	95% CI	32.8 - 61.1	31.8 - 56.1		
p (age)			0.08	0.01	
LV-COi (l/m ² *min)	Total	Mean±SD or median [IQR]	3.2 ± 0.8	3.0 [2.6,3.6]	0.56
		95% CI	1.8 - 4.7	2.2 - 4.5	
	A	Mean±SD	3.6 ± 0.7 [#]	3.3 ± 0.7	0.22
		95% CI	2.4 - 4.7	2.4 - 4.3	
	B	Mean±SD	3.2 ± 0.8	3.0 ± 0.4	0.18
		95% CI	2.1 - 4.6	2.3 - 3.7	
	C	Mean±SD	3.3 ± 0.8	3.4 ± 0.8 [#]	0.60
95% CI		1.8 - 5.0	2.2 - 5.0		
D	Mean±SD	2.8 ± 0.8 [□]	2.9 ± 0.5 [§]	0.57	
	95% CI	1.0 - 4.4	2.2 - 4.1		
p (age)			0.01	0.01	
LV-EF (%)	Total	Mean±SD	67.2 ± 5.4	70.2 ± 4.3	<0.0001
		95% CI	55.6 - 77.3	61.7 - 79.7	
	A	Mean±SD	65.7 ± 4.6	69.8 ± 2.3	0.0002
		95% CI	56.1 - 75.5	65.6 - 73.5	
	B	Mean±SD	67.3 ± 4.0	69.3 ± 3.9	0.07
		95% CI	61.9 - 74.3	61.3 - 76.4	
	C	Mean±SD	68.5 ± 5.9	70.3 ± 5.2	0.28
95% CI		53.1 - 79.6	58.4 - 81.0		
D	Mean±SD	67.4 ± 6.6	71.4 ± 4.9	0.02	
	95% CI	54.2 - 79.3	63.2 - 80.1		
p (age)			0.32	0.37	

B)	Group		Male	Female	p (sex)
LV-CMi (g/m ²)	Total	Mean±SD 95% CI	50.7 ± 6.9 38.2 - 65.9	40.7 ± 5.6 32.1 - 52.1	<0.0001
	A	Mean±SD or median [IQR] 95% CI	51.4 ± 6.4 37.6 - 65.7	40.5 [36.6,44.4] 33.3 - 55.0	<0.0001
	B	Mean±SD 95% CI	49.7 ± 7.2 36.8 - 64.5	39.4 ± 5.2 30.0 - 50.8	<0.0001
	C	Mean±SD 95% CI	53.2 ± 6.6 43.6 - 67.2	41.0 ± 6.4 31.6 - 55.7	<0.0001
	D	Mean±SD 95% CI	48.3 ± 6.7 39.3 - 65.1	41.0 ± 4.7 33.4 - 47.9	<0.0001
	p (age)		0.07	0.61	
LV-TPMi (g/m ²)	Total	Mean±SD 95% CI	23.0 ± 4.7 14.7 - 35.1	18.2 ± 3.1 12.8 - 24.0	<0.0001
	A	Mean±SD 95% CI	22.4 ± 3.8 16.5 - 31.1	17.7 ± 2.8 12.9 - 22.7	<0.0001
	B	Mean±SD 95% CI	22.9 ± 4.4 14.0 - 34.0	18.8 ± 3.2 13.1 - 25.5	0.0004
	C	Mean±SD 95% CI	23.7 ± 5.0 16.0 - 36.1	17.8 ± 2.3 13.1 - 21.1	<0.0001
	D	Mean±SD 95% CI	23.1 ± 5.5 11.9 - 35.7	18.3 ± 3.9 10.5 - 27.2	0.0008
	p (age)		0.82	0.59	
LV-TPMi/ LV-CMi (%)	Total	Mean±SD 95% CI	46.0 ± 9.8 28.6 - 64.2	45.4 ± 8.8 30.1 - 66.2	0.66
	A	Mean±SD 95% CI	43.9 ± 6.9 33.1 - 58.0	43.5 ± 7.0 30.1 - 55.4	0.85
	B	Mean±SD 95% CI	46.8 ± 10.1 29.2 - 71.9	48.3 ± 9.2 30.1 - 65.9	0.57
	C	Mean±SD 95% CI	44.9 ± 9.6 28.3 - 63.8	44.5 ± 6.9 32.0 - 56.5	0.86
	D	Mean±SD 95% CI	48.3 ± 12.0 27.2 - 77.1	45.2 ± 11.2 30.2 - 72.0	0.35
	p (age)		0.39	0.24	
LV-CMi/ LV-EDVi (g/ml)	Total	Mean±SD 95% CI	0.74 ± 0.1 0.56 - 0.96	0.64 ± 0.09 0.49 - 0.85	<0.0001
	A	Mean±SD 95% CI	0.71 ± 0.09 0.56 - 0.88	0.61 ± 0.07 [#] 0.45 - 0.71	<0.0001
	B	Mean±SD 95% CI	0.74 ± 0.13 0.54 - 1.12	0.61 ± 0.07 [#] 0.49 - 0.74	0.0001
	C	Mean±SD 95% CI	0.75 ± 0.09 0.57 - 0.94	0.62 ± 0.08 [#] 0.48 - 0.77	<0.0001
	D	Mean±SD 95% CI	0.75 ± 0.09 0.60 - 0.99	0.70 ± 0.10 ^{□ & §} 0.52 - 0.87	0.07
	p (age)		0.43	<0.001	
LV-TPMi/ LV-EDVi (g/ml)	Total	Median[IQR] 95% CI	0.32[0.28,0.39] 0.22 - 0.50	0.28 [0.25,0.31] 0.20 - 0.42	<0.0001
	A	Mean±SD 95% CI	0.31 ± 0.06 0.22 - 0.47	0.26 ± 0.04 [#] 0.18 - 0.36	0.004
	B	Mean±SD or median [IQR] 95% CI	0.32[0.28,0.38] 0.24 - 0.49	0.29 ± 0.05 0.19 - 0.39	0.02
	C	Mean±SD or median [IQR] 95% CI	0.34 ± 0.08 0.22 - 0.52	0.26 [0.25,0.28] [#] 0.22 - 0.39	0.0017
	D	Mean±SD 95% CI	0.36 ± 0.08 0.22 - 0.59	0.32 ± 0.08 ^{□ §} 0.20 - 0.47	0.05
	p (age)		0.14	0.01	

Changes in LV parameters with age

Regarding the changes in LV volumetric and functional parameters, LV-EDVi, LV-ESVi, LV-SVi, and LV-COi decreased with age: Group A had the highest values and Group D had the lowest values in both males and females (**Table 4A**). Although LV-EF did not significantly differ between the groups, it showed a weak positive correlation with age ($r=0.14$, $p=0.04$). In the analysis of the changes in myocardial masses, LV-TPMi, LV-CMi, and their ratios did not differ between age groups in males or females. In contrast, LV-CMi/LV-EDVi and LV-TPMi/LV-EDVi were altered between the age groups, showing an increase with age in both males and females (**Table 4B**).

Correlations between TPM and phenotype characteristics

In the analysis of the relationship between LV-TPMi and the phenotypic characteristics of the total population, except age and LV-COi, all of the observed parameters correlated with LV-TPMi. Its strongest relationship was with LV-CMi, followed by BSA, LV-ESVi, and LV-EDVi (**Figure 8**). After dividing the population by sex and age, most of these relationships lost their significance (**Table 5**). Notably, a negative correlation between LV-TPMi and LV-EF was observed, independent of sex, in all age groups.

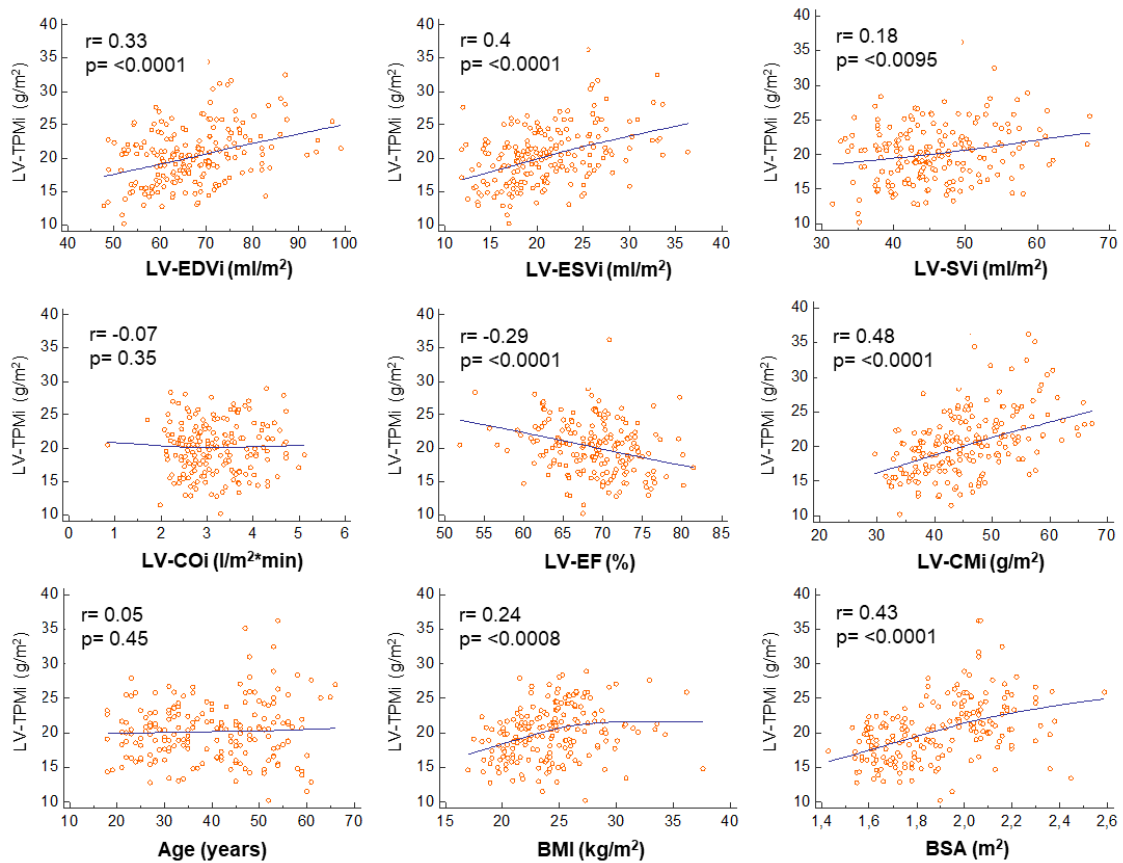


Figure 8 – Correlations of left ventricular (LV) parameters, demographic and other patient characteristics with trabeculated and papillary muscles in the total healthy population, derived with Spearman’s rank correlation analyses (102).

(LV-EDVi: LV end-diastolic volume index; LV-ESVi: LV end-systolic volume index; LV-SVi: LV stroke volume index; LV-COi: LV cardiac output index; LV-EF: LV ejection fraction; LV-CMi: LV end-diastolic compacted myocardial mass index; LV-TPMi: LV end-diastolic papillary and trabeculated muscle mass index; BMI: body mass index; BSA: body surface area; r: correlation coefficient)

Table 5 – Correlations of left ventricular (LV) parameters with trabeculated and papillary muscles by age group, derived with Spearman’s rank correlation analyses (102).

(LV-EDVi: LV end-diastolic volume index; LV-ESVi: LV end-systolic volume index; LV-SVi: LV stroke volume index; LV-COi: LV cardiac output index; LV-EF: LV ejection fraction; LV-CMi: LV end-diastolic compacted myocardial mass index; LV-TPMi: LV end-diastolic papillary and trabeculated muscle mass index; BMI: body mass index; BSA: body surface area; r: correlation coefficient)

* $p < 0.05$

		LV-TPMi			
		Group A	Group B	Group C	Group D
		r	r	r	r
LV-EDVi (ml/m ²)	Male	0.28	0.41*	0.05	0.47*
	Female	0.35	0.21	0.36	0.04
LV-ESVi (ml/m ²)	Male	0.36	0.35	0.27	0.46*
	Female	0.18	0.2	0.52*	0.06
LV-SVi (ml/m ²)	Male	0.15	0.37	-0.08	0.28
	Female	0.37	0.13	0.05	0.02
LV-COi (l/m ² *min)	Male	-0.11	-0.04	-0.4	0.16
	Female	0.01	-0.02	0.04	-0.34
LV-EF (%)	Male	-0.26	-0.12	-0.22	-0.21
	Female	-0.05	-0.15	-0.45*	-0.002
LV-CMi (g/m ²)	Male	0.39	0.18	-0.2	0.26
	Female	0.35	0.21	0.43*	0.03
BMI (kg/m ²)	Male	0.007	-0.3	0.06	-0.19
	Female	0.33	-0.08	0.01	0.26
BSA (m ²)	Male	0.11	-0.26	0.06	0.04
	Female	0.35	-0.04	0.28	0.1
Age (year)	Male	-0.16	0.07	0.18	-0.007
	Female	0.19	-0.07	0.09	-0.08

4.2. Results of the “MR-specific characteristics of left ventricular noncompaction and dilated cardiomyopathy” study

Interobserver variability

The ICC was calculated for all LV parameters and strain values on 15 (48%) and 15 (36%) randomly selected LVNC and DCM patients with excellent values. In the LVNC group ICC values with 95% confident interval were: LV-EDVi: 0.98 (0.95–0.99); LV-ESVi: 0.99 (0.96–0.99); LV-SVi: 0.96 (0.86–0.99); LV-EF: 0.95 (0.83–0.98); LV-TMi: 0.98 (0.93–0.99); LV-TPMi: 0.94 (0.77–0.98); LV-GLS: 0.98 (0.91–0.99); LV-GCS: 0.90 (0.52–0.98). In the DCM group they were: LV-EDVi: 0.98 (0.90–0.99); LV-ESVi: 0.98 (0.92–0.99); LV-SVi: 0.93 (0.82–0.97); LV-EF: 0.95 (0.88–0.98); LV-TMi: 0.97 (0.91–0.99); LV-TPMi: 0.94 (0.85–0.98); LV-GLS: 0.98 (0.94–0.99); LV-GCS: 0.91 (0.74–0.97).

Comparison of the measured LV parameters

In the comparison of the LV volumetric, functional and myocardial mass values, only LV-TPMi and the LV-TPMi/LV-CMi ratio differed significantly between the DCM and LVNC groups, in LVNC group these values were higher. Meanwhile, comparing controls to DCM and LVNC patients, all the studied parameters differed significantly (**Table 6**).

Table 6 – Comparison of the left ventricular (LV) volumetric, functional, and myocardial mass values of the dilated cardiomyopathy, left ventricular noncompaction, and control groups (103). ANOVA with Tukey's post hoc test was used to compare the groups in the case of normal distribution, while Kruskal–Wallis test with Dunn's test was used with non-normally distributed variables. Chi-square tests were used to compare the distributions of categorical data. Values are presented as mean \pm SD or n (%).

(DCM: dilated cardiomyopathy; LVNC: left ventricular noncompaction; C: controls; LV-EDVi: LV end-diastolic volume index; LV-ESVi: LV end-systolic volume index; LV-SVi: LV stroke volume index; LV-EF: ejection fraction; LV-CMi: LV end-diastolic compacted myocardial mass index; LV-TPMi: LV end-diastolic papillary and trabeculated muscle mass index)

	DCM	LVNC	C	p (DCM vs. LVNC)	p (DCM vs. C)	p (LVNC vs. C)
LV-EDVi (ml/m ²)	112.9 \pm 32.3	115.6 \pm 30.3	65.0 \pm 9.7	0.89	<0.0001	<0.0001
LV-ESVi (ml/m ²)	75.5 \pm 28.5	79.2 \pm 30.0	20.4 \pm 4.9	0.73	<0.0001	<0.0001
LV-SVi (ml/m ²)	37.8 \pm 8.2	36.9 \pm 10.2	44.6 \pm 7.9	0.97	0.003	<0.0001
LV-EF (%)	34.6 \pm 7.9	33.2 \pm 10.4	68.5 \pm 6.1	0.78	<0.0001	<0.0001
LV-CMi (g/m ²)	71.1 \pm 20.7	69.8 \pm 15.6	45.7 \pm 7.1	0.92	<0.0001	<0.0001
LV-TPMi (g/m ²)	43.2 \pm 8.9	51.6 \pm 13.6	22.2 \pm 5.5	0.002	<0.0001	<0.0001
LV-TPMi/ LV-CMi	0.64 \pm 0.1	0.74 \pm 0.1	0.48 \pm 0.1	<0.001	<0.0001	<0.0001
LGE n (%)	20 (71)	22 (63)	0 (0)	0.76	-	-
LBBB n (%)	18 (58)	18 (43)	0 (0)	0.20	-	-
Septal LGE in LBBB n (%)	10 (56)	6 (33)	0 (0)	0.18	-	-

Regarding the LV myocardial wall thicknesses, LVNC patients had regionally thinner compact myocardium in the predilection segments of noncompaction (apical and mid segments) in contrast to DCM. Interestingly, LVNC patients differed significantly from healthy subjects in most of the myocardial segments, while only sporadic significance was observed between DCM and control groups (**Table 7**).

Table 7 – Left ventricular wall thicknesses (mm) in dilated cardiomyopathy, left ventricular noncompaction, and controls, compared with ANOVA and Tukey's post hoc test (103). Values are presented as mean ± SD.

(DCM: dilated cardiomyopathy; LVNC: left ventricular noncompaction; C: control group)

		DCM	LVNC	C	p (DCM vs. LVNC)	p (DCM vs. C)	p (LVNC vs. C)
BASAL	1 Anterior	6.6±1.2	6.2±1.2	7.3±1.1	0.32	0.06	0.0001
	2 Anteroseptal	7.3±1.1	7.3±1.2	8.9±1.2	1.00	0.0001	0.0001
	3 Inferoseptal	7.5±1.4	7.0±1.0	7.7±1.0	0.16	0.80	0.02
	4 Inferior	6.5±1.3	6.3±1.2	6.9±1.2	0.77	0.33	0.06
	5 Inferolateral	6.7±1.5	6.3±1.2	7.6±1.3	0.42	0.01	0.0001
	6 Anterolateral	6.7±1.5	6.0±1.2	7.0±1.0	0.07	0.58	0.002
	Mean	6.9±0.4	6.5±0.5	7.6±0.7	0.52	0.13	0.02
MID- VENTRICULAR	7 Anterior	6.1±1.2	5.4±0.9	6.1±1.1	0.01	1.00	0.004
	8 Anteroseptal	7.2±1.5	6.5±1.1	7.5±1.1	0.06	0.52	0.001
	9 Inferoseptal	7.2±1.5	7.1±1.2	7.5±1.2	0.91	0.70	0.39
	10 Inferior	6.3±1.4	5.8±1.1	6.5±1.3	0.16	0.67	0.01
	11 Inferolateral	6.5±1.4	5.1±1.3	6.3±1.1	0.0001	0.70	0.0001
	12 Anterolateral	6.1±1.6	4.6±1.1	6.2±1.0	0.0001	0.98	0.0001
	Mean	6.6±0.5	5.7±0.9	6.7±0.7	0.15	0.96	0.09
APICAL	13 Anterior	5.2±1.1	4.1±0.9	5.8±1.0	0.0001	0.02	0.0001
	14 Septal	6.0±1.3	5.3±1.1	6.1±1.1	0.02	0.81	0.002
	15 Inferior	5.3±1.1	4.4±1.0	5.3±1.2	0.004	1.00	0.002
	16 Lateral	5.3±1.4	3.6±0.7	5.7±1.1	0.0001	0.30	0.0001
	Mean	5.4±0.4	4.3±0.7	5.7±0.3	0.03	0.73	0.01
p (basal vs. mid-ventricular)		0.46	0.21	0.07			
p (mid-ventricular vs. apical)		0.01	0.03	0.08			
p (basal vs. apical)		0.001	0.001	0.001			

Global and segmental strain values

Comparing the groups' LV global strain parameters no significant difference was observed between DCM and LVNC patients, while the controls differed significantly from both LVNC and DCM groups (**Figure 9a**).

Regarding the average LV segmental strain values of basal, mid and apical segments, there were no differences in the longitudinal strains between the LVNC and DCM groups. The apical-third segmental circumferential strain values were significantly worse (less negative: DCM vs. LVNC-R: -30.5% vs. -24.5%, $p=0.048$) and the apical/basal ratio was also significantly lower in the LVNC group than in the DCM group. In contrast, the control population differed significantly from both the LVNC and DCM groups in each basal, mid and apical segments (**Figure 9b**).

In studying the relation of the strain values of each LV third to each other in the groups, we observed similar longitudinal and circumferential strain patterns. The longitudinal strains were the highest in the LV mid-segments, and the lowest in the apical segments with significant differences in each group. Nonetheless, the circumferential strain value of the apical segments differed significantly from the mid and basal LV parts in all populations (**Figure 9c**).

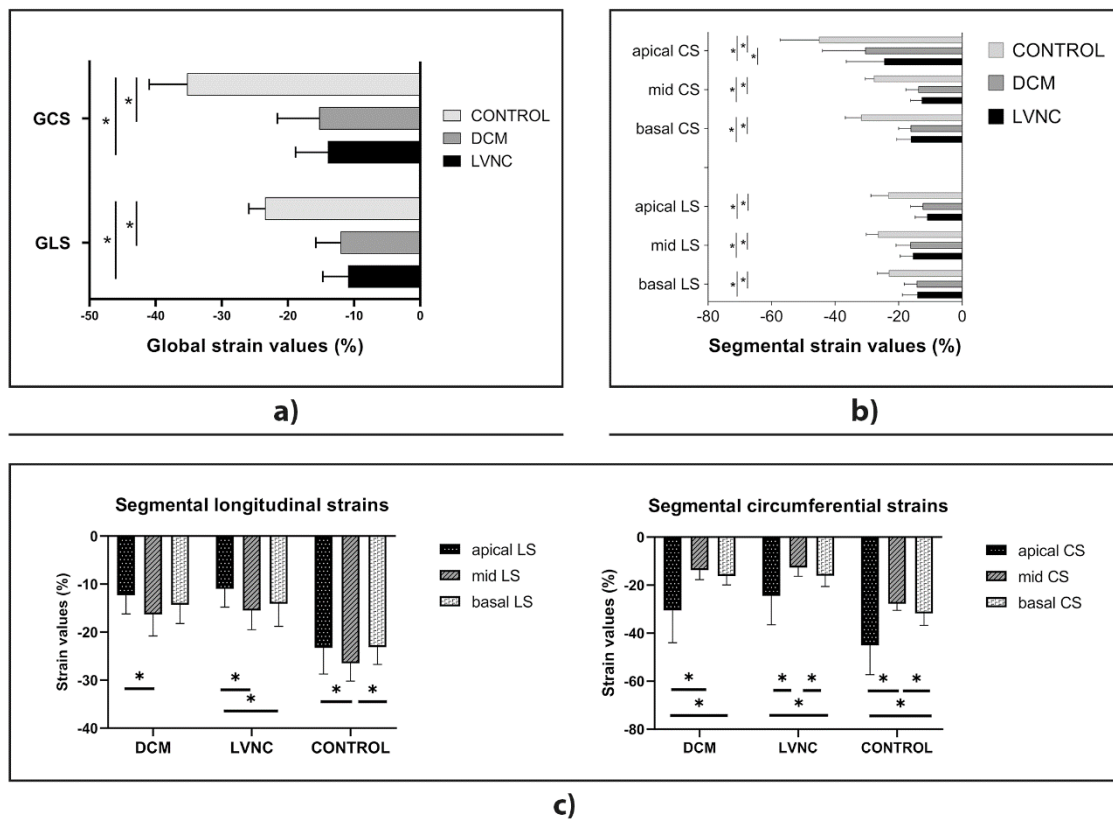


Figure 9 – Interpretation of left ventricular global strain values (a) and segmental strain values between the patient groups (b) and within the patient groups, respectively (c) (103).

ANOVA with Tukey's post hoc test was used to compare the groups in the case of normal distribution, while the Kruskal–Wallis test with Dunn's test was used in the case of non-normally distributed variables.

(DCM: dilated cardiomyopathy; LVNC: left ventricular noncompaction; GCS: global circumferential strain; GLS: global longitudinal strain; apical LS: average apical longitudinal strain; mid LS: average mid ventricular longitudinal strain; basal LS: average basal longitudinal strain; apical CS: average apical circumferential strain; mid CS: average mid ventricular circumferential strain; basal CS: average basal circumferential strain)

* $p < 0.05$

Left bundle branch block and late gadolinium enhancement

LBBB was detected in 18/31 (58%) of DCM and 18/42 (43%) of LVNC patients, however, the difference was nonsignificant. LBBB was not described in the control group, since it was an exclusion criterion.

Contrast agent was used in 63/73 (86%, DCM n=28) of the DCM and LVNC population. LGE was present in 20/28 (71%) of the DCM population and 22/35 (63%) of the LVNC patients with a nonischemic pattern (**Table 6**). Regarding the segmental distribution of mid-wall LGE, the most frequently affected area was the septal part in both diseases. There were no significant regional differences between the patient groups (**Table 8**). Furthermore, more DCM patients with LBBB showed septal LGE than those with LVNC with LBBB, however, the difference was nonsignificant (**Table 6**).

Table 8 – Comparison of segmental distribution of mid-wall LGE in DCM and LVNC patients, Chi-squared test (103). Values are presented as n (%).

(LGE: late gadolinium enhancement; DCM: dilated cardiomyopathy; LVNC: left ventricular noncompaction)

	Contrast agent in DCM (n=28)	Contrast agent in LVNC (n=35)	p (DCM vs. LVNC)
Total number of patients showing LGE n (%)	20 (71)	22 (63)	0.47
Antero-septal wall n (%)	2 (10)	4 (18)	0.57
Infero-septal wall n (%)	1 (5)	1 (5)	0.87
Total septal wall n (%)	14 (70)	13 (59)	0.31
Upper and lower insertion zone n (%)	1 (5)	1 (5)	0.87
Lower insertion zone only n (%)	1(5)	4 (18)	0.25
Anterior n (%)	2 (10)	0 (0)	0.11
Antero-lateral wall n (%)	1 (5)	0 (0)	0.26
Inferior wall n (%)	2 (10)	1 (5)	0.43
Infero-lateral wall n (%)	0 (0)	2 (9)	0.20

Correlations

Regarding the correlations in the trabeculated myocardium, LV-TPMi showed a strong positive correlation with LV-EDVi, LV-ESVi, LV-CMi, and a moderately positive correlation with global strain values in both the DCM and LVNC groups. Interestingly a negative correlation between LV-TPMi and LV-EF was observed in these groups. While the volumetric and myocardial mass values correlated positively, there was no relationship between functional parameters and LV-TPMi in the control group. LV-EDVi, LV-ESVi, LV-GLS, and LV-GCS values increased as LV-EF decreased, while the LV-GCS correlated positively with apical circumferential strain values in all groups. In contrast LV-TPMi showed a weak, but significant correlation with both the apical/basal ratio of the segmental circumferential strain values and the SD-TTP-CS only in LVNC patients. Moreover, SD-TTP-CS showed a moderately negative correlation with LV-EF only in the LVNC group. The LV-TPMi-to-LV-CMi ratio presented a weak positive correlation with LV-GCS in the LVNC and control groups but not in the DCM group (**Table 9**).

Table 9 – The most relevant correlations of the measured left ventricular (LV) parameters assessed with the Pearson correlation coefficient (103).

(DCM: dilated cardiomyopathy; LVNC: LV noncompaction; LV-EDVi: LV end-diastolic volume index; LV-ESVi: LV end-systolic volume index; LV-EF: LV ejection fraction; LV-CMi: LV end-diastolic compacted myocardial mass index; LV-TPMi: LV end-diastolic papillary and trabeculated muscle mass index; LV-GLS: LV global longitudinal strain; LV-GCS: LV global circumferential strain; apical CS: average LV apical circumferential strain; basal CS: average LV basal circumferential strain; SD-TTP-CS: circumferential mechanical dispersion)

* $p < 0.05$, ** $p < 0.0001$

	DCM	LVNC	CONTROL
LV-TPM			
LV-EDVi	0.76**	0.69**	0.40*
LV-ESVi	0.73**	0.76**	0.45*
LV-EF	-0.47*	-0.68**	-0.23
LV-CMi	0.76**	0.83**	0.43*
LV-GLS	0.43*	0.59**	0.09
LV-GCS	0.41*	0.38**	0.23
apicalCS/basalCS	0.14	0.33*	0.03
SD-TTP-CS	0.17	0.35*	0.04
LV-EF			
LV-GLS	-0.83**	-0.85**	-0.78**
LV-GCS	-0.70**	-0.53**	-0.58**
LV-EDVi	-0.66**	-0.62**	-0.68*
LV-ESVi	-0.81**	-0.82**	-0.77**
SD-TTP-CS	-0.31	-0.40*	-0.13
LV-GCS			
apicalCS	0.54*	0.61**	0.62**
SD-TTP-CS	0.20	0.46*	0.32*
LV-TPMi/ LV-CMi	0.08	0.32*	0.41*

Rotational patterns

Observing the rotational patterns, the frequencies of the non-RBR (normal and reverse rotation) and RBR patterns were comparable in all groups (**Figure 10**). Interestingly, all rotational patterns (normal rotation (-/+), reverse rotation (+/-), and positive (+/+) or negative (-/-) RBR) were present in the control group, while reverse rotation was not observed in DCM or LVNC patients (**Table 10**). Regarding the direction of the RBR, a positive RBR was significantly more frequent in controls than in DCM or LVNC patients. Moreover, a negative RBR was observed more frequently in DCM or LVNC group than a positive RBR ($p=0.007$ and $p<0.0001$, respectively). Regarding the frequency of the negative RBR pattern, there were no significant differences between the groups (**Table 10**).

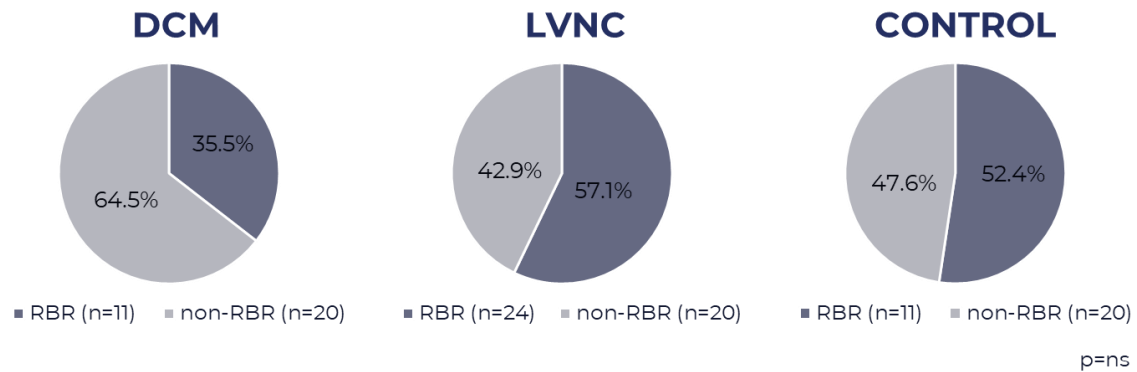


Figure 10 – The frequency of rigid body rotation (RBR) in the studied groups. (DCM: dilated cardiomyopathy; LVNC: left ventricular noncompaction)

Table 10 – Rotational patterns of the studied groups, Chi-squared test (103). Values are presented as n (%). (DCM: dilated cardiomyopathy; LVNC: left ventricular noncompaction) & $p < 0.05$ DCM vs. Control; # $p < 0.05$ LVNC vs. Control

	DCM (n=31)	LVNC (n=42)	CONTROL (n=42)
normal rotation (-/+) n (%)	20 (65)	18 (43)	16 (38)
reverse rotation (+/-) n (%)	0 (0)	0 (0) #	4 (10) #
negative rigid body rotation (-/-) n (%)	10 (32)	22 (52)	13 (31)
positive rigid body rotation (+/+) n (%)	1 (3) &	2 (5) #	9 (21) &#

4.3. Results of the “Right ventricle in left ventricular noncompaction with reduced ejection fraction” study

Interobserver variability

Excellent interobserver agreement values were measured on 15 randomly selected LVNC-R, LVNC-N and DCM patients for all RV parameters. The ICCs with 95% confidence intervals were as follows: RV-EDVi: 0.988 (0.966-0.996); RV-ESVi: 0.996 (0.987-0.998); RV-SVi: 0.931 (0.812-0.976); RV-EF: 0.972 (0.919-0.990); RV-TMi: 0.989 (0.968-0.996); RV-TPMi: 0.965 (0.728-0.991); RV-GLS: 0.900 (0.735-0.965); RV-FWS: 0.919 (0.776-0.972); RV-SS: 0.856 (0.623-0.950).

The usage of contrast agent

Contrast agent was used for 100/119 (84%) of the studied patients, and LGE with a nonischemic pattern was present in 20/28 (71%) of the DCM, 23/36 (64%) of the LVNC-R and 1/36 (3%) of the LVNC-N group.

Left ventricular parameters and clinical features

All the LV parameters differed between the noncompaction groups, while the LVNC-R and DCM groups differed significantly only in LV-TPMi. LV-TPMi correlated negatively with LV-EF (LVNC-R: $r=-0.680$, $p=0.0001$; DCM: $r=-0.431$, $p=0.016$; LVNC-N: $r=-0.434$, $p=0.003$). The LVNC-N group had significantly better LV-GLS and LV-GCS values than the reduced-EF group (**Table 11**).

From the observed clinical features, heart failure, documented arrhythmias, ECG abnormalities, and thromboembolic events were more frequent in LVNC-R and DCM groups with significant differences compared to LVNC-N patients (**Table 12**).

Table 11 – Left ventricular parameters of the dilated cardiomyopathy and left ventricular noncompaction groups (104). ANOVA with Tukey's post hoc test or Kruskal–Wallis test with Dunn's test was used to compare the groups, as appropriate. Values are presented as mean \pm SD.

(DCM: dilated cardiomyopathy; LV: left ventricular; LVNC-R: LV noncompaction with reduced LV function; LVNC-N: LV noncompaction with good LV function; LV-EDVi: LV end-diastolic volume index; LV-ESVi: LV end-systolic volume index; LV-SVi: LV stroke volume index; LV-EF: LV ejection fraction; LV-TPMi: LV trabecular and papillary muscle mass index; LV-CMi: LV compact myocardial mass index; LV-GLS: LV global longitudinal strain; LV-GCS: LV global circumferential strain)

	DCM (n=31)	LVNC-R (n=44)	LVNC-N (n=44)	P (LVNC-R vs. DCM)	P (LVNC-R vs. LVNC-N)	P (DCM vs. LVNC-N)
LV-EDVi (ml/m ²)	112.9 \pm 32.3	114.2 \pm 30.5	74.9 \pm 13.8	0.77	0.0001	0.0001
LV-ESVi (ml/m ²)	75.5 \pm 28.5	78.1 \pm 29.9	26.6 \pm 7.8	0.78	0.0001	0.0001
LV-SVi (ml/m ²)	37.4 \pm 8.2	36.6 \pm 10.1	48.5 \pm 8.0	0.92	0.0001	0.0001
LV-EF (%)	34.6 \pm 7.9	33.4 \pm 10.2	65.0 \pm 5.9	0.81	0.0001	0.0001
LV-TPMi (g/m ²)	43.6 \pm 9.7	51.3 \pm 13.4	28.0 \pm 8.0	0.01	0.0001	0.0001
LV-CMi (g/m ²)	71.1 \pm 20.7	69.2 \pm 15.5	50.4 \pm 11.8	0.87	0.0001	0.0001
LV-GLS (%)	-10.9 \pm 3.8	-12.1 \pm 3.7	-21.3 \pm 2.2	0.29	0.0001	0.0001
LV-GCS (%)	-15.3 \pm 6.3	-14.0 \pm 4.8	-30.2 \pm 5.1	0.59	0.0001	0.0001

Table 12 - Clinical features of the studied groups, compared with Chi-squared test (104). Values are presented as n (%).

(DCM: dilated cardiomyopathy; LVNC-R: left ventricular noncompaction with reduced left ventricular function; LVNC-N: left ventricular noncompaction with good left ventricular function; ECG: electrocardiogram)

	DCM (n=31)	LVNC-R (n=44)	LVNC-N (n=44)	P (LVNC-R vs. DCM)	P (LVNC-R vs. LVNC- N)	P (DCM vs. LVNC-N)
Heart failure n (%)	20 (65)	31 (71)	0 (0)	0.59	0.0001	0.0001
Palpitation n (%)	11 (36)	8 (18)	11 (25)	0.09	0.21	0.59
Documented arrhythmia n (%)	18 (58)	23 (52)	11 (25)	0.62	0.02	0.01
Syncope n (%)	6 (19)	8 (18)	5 (11)	0.90	0.37	0.34
ECG abnormalities n (%)	20 (65)	30 (68)	4 (9)	0.74	0.0001	0.0001
Thromboembolic event n (%)	6 (19)	13 (30)	2 (5)	0.32	0.002	0.04
Sudden cardiac death n (%)	2 (7)	2 (5)	0 (0)	0.72	0.15	0.09
Positive family history n (%)	12 (39)	9 (21)	16 (36)	0.08	0.10	0.84

Right ventricular parameters

The RV volumetric parameters were similar in the LVNC-R and DCM patients, while the LVNC-N group had significantly higher RV-EDVi and RV-SVi values than the other groups. The RV-EF was in the normal range and was comparable in all groups. No significant differences were observed in either RV-TPMi or RV-CMi between the groups (**Table 13**).

Regarding the deformation analysis, nonsignificant differences were found in the RV-GLS and RV-FWS between the reduced-LV-function groups; however, there were relevant differences between the good- and decreased LV-EF populations. RV-SS differed significantly only between the noncompacted groups (**Table 13**).

Table 13 - Right ventricular parameters of the dilated cardiomyopathy and left ventricular noncompaction populations (104). ANOVA with Tukey's post hoc test or Kruskal–Wallis test with Dunn's test was used to compare the groups, as appropriate. Values are presented as mean \pm SD.

(DCM: dilated cardiomyopathy; RV: right ventricular; LVNC-R: left ventricular noncompaction with reduced left ventricular function; LVNC-N: left ventricular noncompaction with good left ventricular function; RV-EDVi: RV end-diastolic volume index; RV-ESVi: RV end-systolic volume index; RV-SVi: RV stroke volume index; RV-EF: RV ejection fraction; RV-TPMi: RV trabecular and papillary muscle mass index; RV-CMi: RV compact myocardial mass index; RV-GLS: RV global longitudinal strain; RV-FWS: RV free-wall strain; RV-SS: RV septal strain)

	DCM (n=31)	LVNC-R (n=44)	LVNC-N (n=44)	p (LVNC-R vs. DCM)	p (LVNC-R vs. LVNC-N)	P (DCM vs. LVNC-N)
RV-EDVi (ml/m ²)	61.0 \pm 17.2	61.0 \pm 16.4	70.8 \pm 15.2	1.00	0.02	0.03
RV-ESVi (ml/m ²)	25.4 \pm 11.5	25.5 \pm 11.8	27.3 \pm 7.3	0.99	0.78	0.78
RV-SVi (ml/m ²)	34.0 \pm 9.2	34.7 \pm 9.5	43.5 \pm 8.0	0.94	<0.0001	<0.0001
RV-EF (%)	57.8 \pm 14.0	58.7 \pm 12.6	61.7 \pm 7.5	0.94	0.43	0.32
RV-TPMi (g/m ²)	22.4 \pm 6.4	23.9 \pm 8.9	22.4 \pm 6.8	0.66	0.63	1.00
RV-CMi (g/m ²)	14.1 \pm 4.4	14.6 \pm 3.8	14.7 \pm 4.2	0.84	0.99	0.81
RV-GLS (%)	-19.8 \pm 5.7	-20.0 \pm 7.1	-24.2 \pm 4.1	0.99	0.003	0.01
RV-FWS (%)	-21.6 \pm 9.1	-23.0 \pm 9.1	-28.3 \pm 5.0	0.72	0.01	0.01
RV-SS (%)	-13.0 \pm 7.3	-11.3 \pm 6.4	-14.1 \pm 4.8	0.48	0.02	0.71

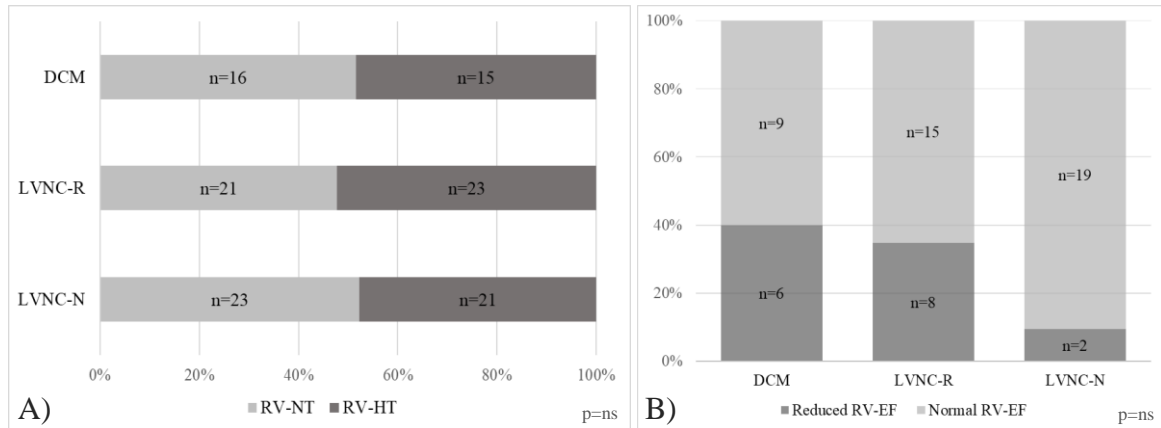


Figure 11 – A) The proportion of patients with normal right ventricular (RV) trabeculation (RV-NT) and with hypertrabeculated RV (RV-HT) in the studied populations and B) reduced RV function in the RV-HT subgroups.

(DCM: dilated cardiomyopathy; LVNC-R: left ventricular noncompaction with reduced left ventricular function; LVNC-N: left ventricular noncompaction with good left ventricular function; RV-EF: RV ejection fraction)

Comparison of the hypertrabeculated and normally trabeculated right ventricle

Dividing the patients by RV trabecular mass, RV-HT was present in equal proportions in the LVNC-N and DCM groups, and more patients showed a higher-than-normal amount of RV trabeculation in the LVNC-R group than in the DCM group, although the difference was nonsignificant (**Figure 11**). However, more patients presented with reduced RV-EF in the DCM group than in the noncompacted groups. In the comparison of the HT and NT subpopulations, not only RV-TPMi but also RV-CMi was significantly higher in the HT groups. There were no differences in the volumetric or functional parameters between the subgroups of the LVNC-N population. In contrast, RV volumetric parameters were significantly higher and RV-EF was significantly lower in the decreased-LV-function groups with RV-HT. The HT subgroup of the LVNC-R population showed significantly worse RV strain values than the NT subgroup (**Figure 12**).

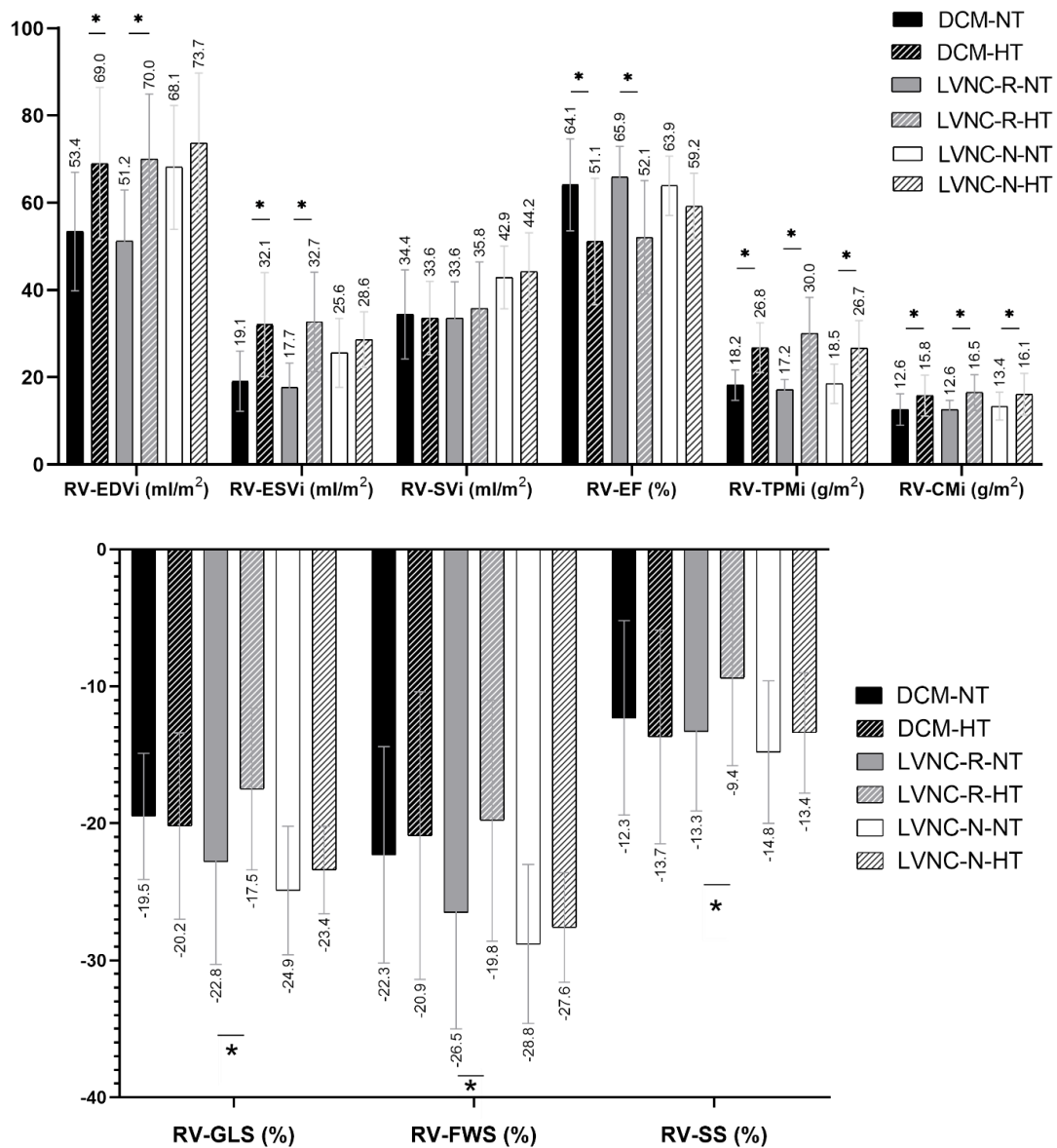


Figure 12 – Comparison of the subgroups with normal right ventricular (RV) trabeculation (NT) and with RV hypertrabeculation (HT) within the groups (104). The independent-samples *t*-test or the Mann–Whitney test was performed to compare the subgroups, as appropriate. Columns present mean \pm SD values.

(DCM-HT: dilated cardiomyopathy with RV hypertrabeculation; DCM-NT: dilated cardiomyopathy with normal RV trabeculation; LVNC-N-HT: left ventricular (LV) noncompaction with good LV function and RV hypertrabeculation; LVNC-N-NT: LV noncompaction with good LV function and normal RV trabeculation; LVNC-R-HT: LV noncompaction with reduced LV function and RV hypertrabeculation; LVNC-R-NT: LV noncompaction with reduced LV function and normal RV trabeculation; RV-CMi: RV

end-diastolic compact myocardial mass index; RV-EDVi: RV end-diastolic volume index; RV-EF: RV ejection fraction; RV-ESVi: RV end-systolic volume index; RV-FWS: RV free-wall strain; RV-GLS: RV global longitudinal strain; RV-SS: RV septal strain; RV-SVi: RV stroke volume index; RV-TPMi: RV end-diastolic trabecular and papillary muscle mass index)

**p < 0.05*

Correlations

RV-TPMi had a strong positive correlation with RV volumes and a negative relationship with RV-EF in all groups. A relevant correlation between LV and RV trabeculation was observed only in the LVNC-N group, while this was not present in the decreased-LV-function groups. RV-EF was correlated with all RV parameters in all the groups, while LV-EF showed a correlation with volumes only in LVNC-R patients (**Table 14**).

The RV strain values showed a moderate correlation with RV-TPMi, LV-TPMi and RV-EF in the LVNC-R group. RV-GLS and RV-FWS correlated negatively with LV-EF in the reduced-LV-function groups, and RV-SS correlated with LV-TPMi, RV-TPMi, RV-EF, RV-EDVi and RV-ESVi only in the LVNC-R group (**Table 14**).

Table 14 – *Correlation coefficients (r) of the right ventricular (RV) parameters, assessed with Pearson's or Spearman's correlation analyses (104).*

A) Correlations between RV parameters and left ventricular (LV) and RV trabeculation

B) Correlations between RV parameters and LV and RV function

C) Correlations between RV strain values and RV volumes

(DCM: dilated cardiomyopathy; LVNC-R: LV noncompaction with reduced LV function; LVNC-N: LV noncompaction with good LV function; RV-EDVi: RV end-diastolic volume index; RV-ESVi: RV end-systolic volume index; RV-SVi: RV stroke volume index; RV-EF: RV ejection fraction; RV-TPMi: RV end-diastolic trabecular and papillary muscle mass index; RV-CMi: RV end-diastolic compact myocardial mass index; RV-GLS: RV global longitudinal strain; RV-FWS: RV free-wall strain; RV-SS: RV septal strain; LV-TPMi: LV end-diastolic trabecular and papillary muscle mass index; LV-EF: LV ejection fraction)

**p < 0.05, **p < 0.0001*

A)	LV-TPMi			RV-TPMi		
	DCM	LVNC-R	LVNC-N	DCM	LVNC-R	LVNC-N
	r			r		
RV-EDVi	0.28	0.37*	0.50*	0.64**	0.71**	0.54**
RV-ESVi	0.06	0.36*	0.44*	0.81**	0.82**	0.65**
RV-SVi	0.41*	0.02	0.40*	0.07	0.11	0.32
RV-EF	0.13	-0.25	-0.20	-0.63*	-0.70**	-0.54**
RV-TPMi	0.23	0.29	0.47*	1	1	1
RV-CMi	0.41*	0.46*	0.38*	0.70**	0.63**	0.71**
RV-GLS	0.24	0.49*	0.13	0.22	0.50*	0.35*
RV-FWS	0.23	0.27	0.10	0.22	0.38*	0.25
RV-SS	-0.04	0.33*	-0.08	0.24	0.45*	0.10

B)	LV-EF			RV-EF		
	DCM	LVNC-R	LVNC-N	DCM	LVNC-R	LVNC-N
	r			r		
RV-EDVi	-0.10	-0.31*	-0.20	-0.37*	-0.60**	-0.37*
RV-ESVi	-0.21	-0.30*	-0.28	-0.81**	-0.87**	-0.63**
RV-EF	0.47*	0.29	0.32*	1	1	1
RV-TPMi	-0.32	-0.20	-0.37*	-0.63**	-0.70**	-0.54**
RV-GLS	-0.59*	-0.50*	-0.23	-0.14	-0.59**	-0.47*
RV-FWS	-0.55*	-0.32*	-0.16	-0.24	-0.44*	-0.21
RV-SS	-0.08	-0.26	0.06	-0.17	-0.46*	-0.27

C)	RV-EDVi			RV-ESVi		
	DCM	LVNC-R	LVNC-N	DCM	LVNC-R	LVNC-N
	r			r		
RV-GLS	0.38*	0.41*	0.30*	0.19	0.53**	0.38
RV-FWS	0.19	0.33*	0.15	0.20	0.34*	0.15
RV-SS	0.29	0.32*	0.02	0.26	0.45*	0.15

5. Discussion

5.1. Discussion of the “Sex- and age-specific normal values of left ventricular parameters with a threshold-based method” study

In contrast to the conventional contouring technique, the implementation of new normal reference ranges are recommended for the TB method. Thus, we described new sex- and age-specific LV parameter values. This accurate evaluation of LV trabeculation is clinically relevant in conditions with physiological and pathological LV hypertrabeculation (105-107).

In the total studied population, in accordance with previously published data with different postprocessing techniques, biometric differences were observed between males and females: males had significantly higher LV volumes and myocardial mass values and lower LV-EF than females (108-110). Previous studies described age-related changes in LV functional parameters, but we did not find information about sex-related differences at different ages (99, 111-114).

It should be emphasized that despite the relatively small number of subgroups, LV-CMi and LV-TPMi differed significantly between males and females in all subgroups. Trabecular quantification was presented previously in the literature: a) as trabecular mass values calculated with the conventional contouring technique, b) with volumetric details, c) with percentiles in healthy participants and patients with cardiac disorders. However, these studies did not stratify the results by age (16, 18-20). Andre et al. and Cai et al. described the LV trabeculation of healthy subjects in different age groups: Andre et al reported the trabecular volumes, while Cai et al. used the fractal analysis (17, 21). We did not find publications focusing on both age- and sex-related changes using the TB trabecular mass quantification method. Since this was the first investigation which assessed age- and sex-specific LV parameters using the TB method, our results would be applicable in the establishment of novel normal reference ranges for LV-TPMi.

Our finding that all LV volumetric parameters decreased with age are in line with other echocardiographic and CMR studies (111, 115-117). As in our investigation, the connection between LV-EF and age is controversial in the literature. Fiechter et al. and Nikitin et al. strengthened this connection, but other studies revealed that aging did not influence the LV function (111, 115-118).

We observed that LV-TPMi and LV-CMi was similar in every age group in both male and female, which might support the accurate and precise patient selection (i.e. elderly people were a healthy population). We did not find data about age-dependent changes in the LV-TPMi calculated with the TB method. We found only one investigation including 140 patients where LV-TPMi decreased with increasing age, which is not comparable to our study, since the papillary muscles were included in the compact myocardial mass (16). It is important to highlight that depending on the analysis software, papillary muscle mass can be counted in either compact or trabeculated muscle mass. This might result in differences between the outcomes of various studies, however, Andre et al. presumed this issue not significant (21).

Regarding the LV-CMi values, controversial results have been reported with increasing age both in echocardiography and CMR investigations (111, 113, 115, 119-122). The studies that reported similar LV myocardial mass values in younger and older population, were confirmed by autopsy (123). This observation is in line with our results. The underlying pathophysiological mechanism could be the age-related loss of myocytes and compensatory reactive cellular hypertrophy, which maintains the total weight of the myocardium (124). In our study, the LV-TPMi/LV-CMi ratio was not significantly different between males and females, which might imply a sex-independent connection between trabecular mass and compact myocardial mass. Furthermore, no changes were observed between the age groups. Another investigation with a conventional contouring technique described similar LV-TPMi/LV-CMi ratios, however they did not stratify this ratio by age (18). Smaller ratios were reported by Fernandez et al. using another contouring method, but they did not study sex and age differences (19). The proposed normal values of the LV-TPMi/LV-CMi ratio might have additive value in the differential diagnosis of conditions with excessive LV trabeculation.

Regarding the mass-to-volume ratios, the difference between males and females in all age groups might be due to the significantly different myocardial mass values of males and females besides the less significant differences in the volumetric parameters. Both the LV-CMi/LV-EDVi and LV-TPMi/LV-EDVi ratios were higher in the elderly due to the unchanged myocardial mass values and the age-dependent decrease in volumetric parameters. These results are in line with the literature (111, 119). A Framingham Offspring cohort with 1294 members was analyzed regarding the connection of age and

the trabeculation-to-EDV ratio (18). In this study, trabeculation was expressed as volume, and contrary to our results, the ratio had a weak negative correlation with age. As the LV mass-to-LV-EDV ratio was applied to distinguish HCM from an athlete's heart in a recent study, the reference ranges for myocardial mass-to-volume ratios might have clinical utility in the differential diagnosis of pathological and physiological conditions associated with hypertrophy or hypertrabeculation (106).

Regarding the correlations, LV-TPMi and age showed no relation in our studied population, suggesting that LV-TPMi remains unchanged over time.

Also, in accordance with our results, Chuang et al. described the correlation of trabeculation and LV mass, although they characterized trabeculae as volumes (18). Janik et al. also described this correlation enrolling a diverse population, not dividing it by sex or age (105). Several studies support our results by observing a strong relationship between LV trabeculation and EDV or ESV, measured either by volume or by myocardial mass (16, 18, 21).

In our study, there was a positive correlation between LV-TPMi and BSA in the total population, but no data were found in the literature about this relationship. In concordance with our results, the lack of connection between LV-TPMi and BMI has also been described (121).

After stratifying the total population by age, the small number of subgroups could be the reason for the lack of correlations between LV-TPMi and volumetric parameters, LV-EF, LV-CMi, BMI, BSA and age.

Interestingly, there was a negative correlation between LV-TPMi and LV-EF, which is corroborated by the study of Bentatou et al. (16). This correspondence might be explained by the association between lower EF and higher myocardial mass (i.e. in males) and by the correlation between LV-CMi and LV-TPMi in our study. In addition, LVNC patients even with good LV function have significantly lower LV-EF compared to healthy people (125). Paun et al. described that an increase in the amount of trabeculation could maintain the SV using lower strains with less energy (3). Moreover, Kawamura et al. investigated the connection between trabeculation and B-type natriuretic peptide and concluded that increased LV trabeculation was associated with LV dysfunction (126).

5.2. Discussion of the “MR-specific characteristics of left ventricular noncompaction and dilated cardiomyopathy” study

As excessive LV trabeculation can be present in many patients with DCM, differentiation from LVNC with decreased LV-EF might be challenging. Thus, our study aimed to describe the similarities and differences between these cardiomyopathies using the TB technique and FT strain analysis (93, 127).

Highlighting the similarities between the DCM and LVNC groups, there were no significant differences in LV volumetric, functional or global strain parameters, in line with previous studies (128-130). As in DCM, the larger LV volumetric parameters in LVNC can be caused by the dilation of the ventricle upon reduced heart function and might become even more pronounced due to the presence of trabeculae (3). Some studies described higher volumes and lower EF in a DCM population compared with LVNC, and this lower LV function in DCM might indicate a discrepancy with our results (131, 132). Regarding the LV global strains, the LV-EF showed a negative correlation with LV-GLS and LV-GCS values. The decreased strains with the worsening of LV function in both LVNC and DCM possibly were caused by cardiomyopathy-related LV remodeling (107, 133). Contrary to our results, another study showed significant difference regarding LV-GLS comparing DCM and LVNC patients (134). This might be explained by the higher difference in LV function between the groups in this study.

Regional myocardial thinning was observed only in LVNC patients, which appears to be more disease-specific than the consequence of impaired LV function. Differences in myocardial wall thicknesses between LV basal, mid and apical segments indicate the higher amount of trabeculation in LVNC and DCM groups. MacIver et al. observed an exponential connection between end-diastolic wall thickness and EF, supporting our observations in LVNC but not in DCM. This deviation might be because of the applied mathematical model fitted for an idealized LV (135).

The morphological characteristics of LVNC resulted not only in thinner compact myocardium but also in higher LV-TPMi values than DCM patients (129-131). Our results are supported by a Framingham Offspring cohort study, in which trabeculated and compact myocardium, as well as LV-TPMi and volumetric parameters showed positive

correlation, while LV-TPMi and EF showed negative correlation (18). Whether excessive trabeculation is part of a compensatory mechanism to decrease ventricular function or whether the decrease in ventricular function causes excessive trabeculation is still controversial. It is important to highlight the positive correlation between LV-TPMi and LV global strains in DCM and LVNC patients. It suggests, that due to trabecula-induced changes in LV structure, the higher trabecular mass value may be associated with worse strain values. Additionally, the positive correlation between LV-TPMi/LV-CMi and LV-GCS in LVNC patients implies the importance of circumferential fibers in noncompaction (3, 17, 97, 107).

Segmental strains in LV basal, mid and apical segments decrease due to the cardiomyopathy-related impairment of ventricular function (107, 136). The relation of the average strain values of the LV basal, mid and apical segments to each other was similar between DCM, LVNC and healthy controls. Segmental longitudinal strains were similar between DCM and LVNC in LV apical, mid and basal segments. In contrast, segmental circumferential strains of the apical segments were decreased but still preserved in LVNC and DCM patients, with significantly worse value in LVNC (137). Circumferential strains have a higher impact on maintaining cardiac function in healthy subjects, and the apex consists of mainly circumferential myocardial fibers (137, 138). These support our finding that the apex had the highest circumferential strain values. Moreover, the strong positive correlation between LV-GCS and apical circumferential strain in our study strengthens this theory. We hypothesize that higher apical circumferential strains compensate for the lower apical longitudinal strains, which arise from the abovementioned anatomical myocardial fiber orientation (i.e., in the apical region, the circumferential fibers are more pronounced, while the longitudinal fibers add less to the function).

The difference in apical circumferential strains between the patient groups can be explained by several reasons. First, it might originate from the abovementioned mechanism, as hypertrabeculation-related structural changes cause lower strain values in LVNC, which is also supported by the positive correlation between LV-TPMi and the apical/basal circumferential strain ratio observed only in LVNC in our study (3). Another possible reason for the reduction of circumferential apical shortening in LVNC could be

the involvement of circumferential myocardial fibers in the midwall, which suggests transmural dysfunction in the trabeculated apical region (138). This transmural involvement and pronounced trabeculation might cause increased circumferential mechanical dispersion, as LV-TPMi correlated positively with SD-TTP-CS only in LVNC patients in our investigation. Moreover, a negative relationship was observed between LV-EF and mechanical dispersion, which might also support the abovementioned correlation between trabeculae and LV function. A further reason for the decreased strains in the apical segments could be the noncompaction-specific, thinner apical compact myocardium, where higher wall stress might generate worse strain values (135).

The prevalence of LBBB and the segmental prevalence of LGE were similar between the studied DCM and LVNC groups. Whether the presence of LBBB in LVNC causes the same changes in volumetric and functional parameters as it does in DCM, or whether LBBB and the mostly septal arrangement of LGE are related to each other, are still unknown (139). These associations need further investigation, as the prognostic role of LGE is known (69, 140).

Although RBR is commonly mentioned in association with LVNC, limited data are available from CMR regarding this issue (130, 141-145). One of our previous investigations also described nonsignificant differences between RBR and non-RBR cases in the groups (107). As for the direction of RBR, our results are consistent with the literature, as decreased LV function has been associated with negative RBR, while positive RBR might be observed in good LV function (84, 107, 130, 146). RBR can be caused by damaged fiber orientation and fibrosis in pathological conditions, as the course of the muscle fibers and the relative displacement of the epicardial and endocardial helices change (147). Normally, basal rotation changes during the maturational process of LV torsion, and the connection of myocardial fibers changes during growth (95, 148). Presumably, defects in this process might lead to persistent RBR in adults without major changes in cardiac morphology. The rotational patterns of the healthy population are controversial, as we found a heterogeneous pattern, while some echocardiographic studies described normal rotation (84, 94).

5.3. Discussion of the “Right ventricle in left ventricular noncompaction with reduced ejection fraction” study

In this study, we described the RV trabeculation and RV functional characteristics of patients with LVNC and decreased LV function.

Describing the characteristics of the LV, the good- and decreased-LV-function groups differed in the volumetric and functional parameters. The only difference between the LVNC-R and DCM populations was in the value of the LV-TPMi, which was consistent with our previous results and with the literature (107, 125, 129-131, 149). Furthermore, according to our previous studies, both LV and RV volumetric, functional, and myocardial mass parameters of a large LVNC population with good LV-EF differed significantly from those of healthy controls (34, 125). For this reason, we did not include a healthy population in this investigation. Nonetheless, these alterations between the healthy population and patients with excessive LV trabeculation and normal LV-EF (i.e. higher volumetric and myocardial mass values, and worse EF and strains in LV hypertrabeculation) might have relevance, especially in conditions with volume overload. It should be highlighted that the term hypertrabeculation covers a wide range of morphological appearances of the myocardium, where it is important to consider the possible subclinical changes (58).

In contrast with the LVNC-N group, the RV volumetric parameters were decreased but still in the normal range in the LVNC-R and DCM groups, which might be due to LV enlargement that compresses the RV through mechanical interactions (150). As potential RV involvement does not necessarily or rapidly develop in LV-affected diseases, RV function is preserved and similar between all groups. Later, if the RV cannot compensate the increasing LV volumes, the RV volumes might become larger and RV-EF might decrease (151-154). The observed strong negative correlations between RV volumes and RV-EF in our study support this hypothesis.

RV-TPMi did not differ significantly between the groups, but did only when divided into NT and HT subpopulations. The correlations of RV-TPMi with RV volumes and RV-EF corroborate the significantly higher volumes and lower RV-EF values observed in the HT subgroups with decreased LV function (72, 153, 155). Although these differences were not present in the LVNC-N group, they were also observed in a larger noncompacted

population with good LV-EF (34). These findings suggest that in the case of RV hypertrabeculation, RV function might deteriorate independently of LV function.

Even with the abovementioned correlations of RV function, volume and hypertrabeculation, it is still a debate whether increased volume causes more extensive trabeculation or vice versa, as these correlations were observed in all three HT subgroups. Notably, the LVNC-R group had the most RV-HT cases, while most patients with decreased RV function were in the DCM-HT subgroup. As we did not find relevant confirming data, a follow-up study on a larger noncompacted population would be necessary to verify these results. In addition, the prognostic role of RV function in DCM was discussed in a study by Gulati et al. (31).

It is worth mentioning that RV and LV trabeculation correlated significantly only in the LVNC-N group (21, 34). Stacey et al. also observed a correlation between the RV apical trabecular thickness and the LV noncompacted-to-compacted ratio even in LVNC patients with reduced EF (153). In contrast, the lack of correlation in the reduced-LV-function groups might be due to the smaller sample size of our study.

As LV-TPMi and LV-EF correlated with RV volumetric parameters only in noncompaction the pathological relevance of the morphological features of LVNC may be found in the RV.

Regarding our results, in the presence of good LV function, all the RV strains were independent of LV trabeculation and LV function. However, once LV function had decreased, both RV-GLS and RV-FWS decreased as well, independently of the etiology. Consistent with this finding, more decreased RV strain values were described in DCM patients with a higher risk of major cardiovascular events combined with other cardiovascular diseases in the literature (156-160).

Not only LV function but also LV trabeculation might have an impact on RV strains: notable correlations were observed between the RV-SS values and LV-TPMi in noncompaction patients with reduced LV-EF. This could have been due to ventricular interdependency, as the septal part is also markedly affected by trabeculation in noncompaction, and LV contraction through the interventricular septum contributes to 20-40% of RV pressure (161).

It is important to highlight, that significant correlations between all measured RV strains and RV trabeculation were observed only in the LVNC-R group. Additionally, significantly lower RV strains were observed in the HT subgroup, than in the NT subgroup solely in LVNC-R population. These results are in line with a larger LVNC study with good LV-EF and, interestingly, were not seen in the DCM group (34). Importantly, RV involvement in LVNC has a worse prognosis based on published data (71, 162). Regarding our results, RV trabeculation might have an impact on the deterioration of RV strains. This would suggest that the HT subgroup of the LVNC-R population is the most affected group, presumably with a worse prognosis. Thus, a more careful follow-up of these patients can be recommended.

6. Limitations

We applied the TB method in all of our studies. The main limitation of this technique is that it is not widely available and not comparable with other trabecular measuring techniques, as their intervendor agreement has not yet been established. In addition, recent volume and EF quantifications use a stack of thick short-axis (SA) slices, and 8–10 mm is typical for Z-direction spatial resolution. Since trabeculae and papillary muscles do not necessarily cross the slice completely perpendicularly, this can cause partial volume effects. Depending on the actual path of the trabeculae, this might influence the TB quantification.

The FT method used in the second and third investigations also has limitations. The lack of accepted validation for this technique and the poorer reproducibility of segmental strains make its utility controversial (92, 163).

Although our first study was conducted on a large cohort, the main limitation was its single-centre setting. In addition, the studied group size decreased after dividing the population by sex and age, which may have affected the statistical findings.

The main limitation of our second and third studies was the sample size of the groups and subgroups since we applied strict patient selection during the enrollment process.

In our third study, a significant difference was found between the two noncompacted groups in age, which may have affected the results slightly. This could be due to the progression of the diseases, as deterioration of LV function might become more pronounced over time.

7. Conclusion

To ensure the precise evaluation and assessment of LV trabeculation, we recommend sex- and age-specific normal values for LV parameters for a healthy population, utilizing the TB trabeculated and papillary muscle mass quantification method. The trabecular and compacted mass values and the trabeculated-to-compacted myocardial mass ratio were independent of age or sex, and the observed correlations support these results. As the TB semiautomatic quantification method applies to evaluating myocardial trabeculation with high reproducibility and better interobserver agreement than the conventional technique, our results might have clinical utility for the differential diagnosis of physiological and pathological conditions with LV hypertrabeculation.

In the following, we used the TB method and FT strain analysis to compare DCM and LVNC patients with reduced LV-EF. Despite their similarities, the significantly higher LV trabecular mass and significantly worse LV apical circumferential strain of LVNC patients might be due to the morphological characteristics of LVNC with hypertrabeculated apical regions. These results could be helpful in the differentiation and risk stratification of these cardiomyopathies.

Finally, we described the RV characteristics of noncompaction and DCM patients. Significant differences between a normal and a hypertrabeculated RV, deteriorated RV strains, and relevant correlations between RV and LV parameters in both LVNC groups were observed. These could suggest the involvement of the RV in conditions with LV hypertrabeculation and might predict worse prognosis of patients with noncompaction and reduced LV function. For this reason, careful follow-up of these patients should be recommended.

To summarize, the most important implications of our study are the following:

1. We determined sex- and age-specific LV-TPMi values with the TB method first in the literature and recommended new reference values for LV parameters. This could help distinguish physiological and pathological trabeculation.

2. LVNC patients with reduced LV function have higher LV trabecular mass and worse LV apical circumferential strain values compared to DCM patients, which might have differential diagnostic relevance.

3. We described RV characteristics of DCM and LVNC patients with reduced LV function. RV involvement in conditions with LV hypertrabeculation might be presumed with prognostic relevance.

8. Summary

Evaluation of trabeculation is quite challenging, and the presence and extent of hypertrabeculation raise differential-diagnostic problems, as there is no universal criterion of the normal amount of trabeculation. LVNC is known for the extended trabecular meshwork in the LV, particularly in the apical region, and RV involvement of the disease is also a recently highlighted issue in cardiac imaging. Our studies investigated LV and RV trabeculation in different cardiac conditions and highlighted the differential diagnoses of LVNC.

In our first study we recommended novel sex- and age-related normal values of LV parameters using the TB method, which is applicable for precise trabecular and papillary mass assessment. We should highlight that LV myocardial mass values were independent from age. Our study may give guidance to determine whether a prominent LV trabeculation is pathological or a normal variant.

Extended LV trabeculation also raises differential diagnostic problems between the genetically and morphologically overlapping LVNC and DCM. In our second and third study, we investigated the characteristics of these cardiomyopathies' LV and RV with the abovementioned TB method and FT strain analysis. Regarding LV parameters, the different LV trabecular mass and LV apical circumferential strain values represent novel aspects of cardiac imaging and ensure clinical utility in differential diagnosis. Regarding the RV, we observed relevant connections between LV and RV parameters and described specific characteristics of the hypertrabeculated RV with worsening strain parameters. These alterations might suggest the involvement of the RV in noncompaction and predict a possible RV functional decrease. Nonetheless, careful follow-up of these patients is suggested.

9. References

1. Braunwald E. Structure and function of the normal myocardium. *Br Heart J*. 1971;33(Suppl):Suppl:3-8.
2. Kawel N, Nacif M, Arai AE, Gomes AS, Hundley WG, Johnson WC, et al. Trabeculated (noncompacted) and compact myocardium in adults: the multi-ethnic study of atherosclerosis. *Circ Cardiovasc Imaging*. 2012;5(3):357-66.
3. Paun B, Bijmens B, Butakoff C. Relationship between the left ventricular size and the amount of trabeculations. *Int J Numer Method Biomed Eng*. 2018;34(3).
4. Dawson DK, Maceira AM, Raj VJ, Graham C, Pennell DJ, Kilner PJ. Regional thicknesses and thickening of compacted and trabeculated myocardial layers of the normal left ventricle studied by cardiovascular magnetic resonance. *Circ Cardiovasc Imaging*. 2011;4(2):139-46.
5. Halaney DL, Sanyal A, Nafissi NA, Escobedo D, Goros M, Michalek J, et al. The Effect of Trabeculae Carneae on Left Ventricular Diastolic Compliance: Improvement in Compliance With Trabecular Cutting. *J Biomech Eng*. 2017;139(3):0310121-8.
6. Sedmera D, Pexieder T, Vuillemin M, Thompson RP, Anderson RH. Developmental patterning of the myocardium. *Anat Rec*. 2000;258(4):319-37.
7. Olejnickova V, Hamor PU, Janacek J, Bartos M, Zabrodska E, Sankova B, et al. Development of ventricular trabeculae affects electrical conduction in the early endothermic heart. *Dev Dyn*. 2022:1-13.
8. Faber JW, D'Silva A, Christoffels VM, Jensen B. Lack of morphometric evidence for ventricular compaction in humans. *J Cardiol*. 2021;78(5):397-405.
9. de Boer BA, van den Berg G, de Boer PA, Moorman AF, Ruijter JM. Growth of the developing mouse heart: an interactive qualitative and quantitative 3D atlas. *Dev Biol*. 2012;368(2):203-13.
10. Luxan G, Casanova JC, Martinez-Poveda B, Prados B, D'Amato G, MacGrogan D, et al. Mutations in the NOTCH pathway regulator MIB1 cause left ventricular noncompaction cardiomyopathy. *Nat Med*. 2013;19(2):193-201.
11. Sedmera D, Reckova M, DeAlmeida A, Coppin SR, Kubalak SW, Gourdie RG, et al. Spatiotemporal pattern of commitment to slowed proliferation in the embryonic mouse heart indicates progressive differentiation of the cardiac conduction system. *Anat Rec A Discov Mol Cell Evol Biol*. 2003;274(1):773-7.
12. Petersen SE, Jensen B, Aung N, Friedrich MG, McMahon CJ, Mohiddin SA, et al. Excessive Trabeculation of the Left Ventricle: JACC: Cardiovascular Imaging Expert Panel Paper. *JACC Cardiovasc Imaging*. 2023;16(3):408-25.
13. Meyer HV, Dawes TJW, Serrani M, Bai W, Tokarczuk P, Cai J, et al. Genetic and functional insights into the fractal structure of the heart. *Nature*. 2020;584(7822):589-94.
14. Miller CE, Wong CL. Trabeculated embryonic myocardium shows rapid stress relaxation and non-quasi-linear viscoelastic behavior. *J Biomech*. 2000;33(5):615-22.
15. Jacquier A, Thuny F, Jop B, Giorgi R, Cohen F, Gaubert JY, et al. Measurement of trabeculated left ventricular mass using cardiac magnetic resonance imaging in the diagnosis of left ventricular non-compaction. *Eur Heart J*. 2010;31(9):1098-104.
16. Bentatou Z, Finas M, Habert P, Kober F, Guye M, Bricq S, et al. Distribution of left ventricular trabeculation across age and gender in 140 healthy Caucasian subjects on MR imaging. *Diagn Interv Imaging*. 2018;99(11):689-98.
17. Cai J, Bryant JA, Le TT, Su B, de Marvao A, O'Regan DP, et al. Fractal analysis of left ventricular trabeculations is associated with impaired myocardial deformation in healthy Chinese. *J Cardiovasc Magn Reson*. 2017;19(1):102.

18. Chuang ML, Gona P, Hautvast GL, Salton CJ, Blease SJ, Yeon SB, et al. Correlation of trabeculae and papillary muscles with clinical and cardiac characteristics and impact on CMR measures of LV anatomy and function. *JACC Cardiovasc Imaging*. 2012;5(11):1115-23.
19. Fernandez-Golfin C, Pachon M, Corros C, Bustos A, Cabeza B, Ferreiros J, et al. Left ventricular trabeculae: quantification in different cardiac diseases and impact on left ventricular morphological and functional parameters assessed with cardiac magnetic resonance. *J Cardiovasc Med (Hagerstown)*. 2009;10(11):827-33.
20. Choi Y, Kim SM, Lee SC, Chang SA, Jang SY, Choe YH. Quantification of left ventricular trabeculae using cardiovascular magnetic resonance for the diagnosis of left ventricular non-compaction: evaluation of trabecular volume and refined semi-quantitative criteria. *J Cardiovasc Magn Reson*. 2016;18(1):24.
21. Andre F, Burger A, Lossnitzer D, Buss SJ, Abdel-Aty H, Gianntisis E, et al. Reference values for left and right ventricular trabeculation and non-compacted myocardium. *Int J Cardiol*. 2015;185:240-7.
22. Captur G, Syrris P, Obianyo C, Limongelli G, Moon JC. Formation and Malformation of Cardiac Trabeculae: Biological Basis, Clinical Significance, and Special Yield of Magnetic Resonance Imaging in Assessment. *Can J Cardiol*. 2015;31(11):1325-37.
23. Samsa LA, Yang B, Liu J. Embryonic cardiac chamber maturation: Trabeculation, conduction, and cardiomyocyte proliferation. *Am J Med Genet C Semin Med Genet*. 2013;163C(3):157-68.
24. Shou W, Aghdasi B, Armstrong DL, Guo Q, Bao S, Charng MJ, et al. Cardiac defects and altered ryanodine receptor function in mice lacking FKBP12. *Nature*. 1998;391(6666):489-92.
25. Chowdhury R, Ashraf H, Melanson M, Tanada Y, Nguyen M, Silberbach M, et al. Mouse Model of Human Congenital Heart Disease: Progressive Atrioventricular Block Induced by a Heterozygous Nkx2-5 Homeodomain Missense Mutation. *Circ Arrhythm Electrophysiol*. 2015;8(5):1255-64.
26. Phoon CK, Acehan D, Schlame M, Stokes DL, Edelman-Novemsky I, Yu D, et al. Tafazzin knockdown in mice leads to a developmental cardiomyopathy with early diastolic dysfunction preceding myocardial noncompaction. *J Am Heart Assoc*. 2012;1(2):jah3-e000455.
27. Haddad F, Hunt SA, Rosenthal DN, Murphy DJ. Right ventricular function in cardiovascular disease, part I: Anatomy, physiology, aging, and functional assessment of the right ventricle. *Circulation*. 2008;117(11):1436-48.
28. Damiano RJ, Jr., La Follette P, Jr., Cox JL, Lowe JE, Santamore WP. Significant left ventricular contribution to right ventricular systolic function. *Am J Physiol*. 1991;261(5 Pt 2):H1514-24.
29. Corrado D, Basso C, Judge DP. Arrhythmogenic Cardiomyopathy. *Circ Res*. 2017;121(7):784-802.
30. Manca P, Nuzzi V, Cannata A, Castrichini M, Bromage DI, De Luca A, et al. The right ventricular involvement in dilated cardiomyopathy: prevalence and prognostic implications of the often-neglected child. *Heart Fail Rev*. 2022;27(5):1795-805.
31. Gulati A, Ismail TF, Jabbour A, Alpendurada F, Guha K, Ismail NA, et al. The prevalence and prognostic significance of right ventricular systolic dysfunction in nonischemic dilated cardiomyopathy. *Circulation*. 2013;128(15):1623-33.

32. Stampfli SF, Gotschy A, Kiarostami P, Ozkartal T, Gruner C, Niemann M, et al. Right ventricular involvement in left ventricular non-compaction cardiomyopathy. *Cardiol J*. 2022;29(3):454-62.
33. Kiss AR, Gregor Z, Furak A, Szabo LE, Dohy Z, Merkely B, et al. Age- and Sex-Specific Characteristics of Right Ventricular Compacted and Non-compacted Myocardium by Cardiac Magnetic Resonance. *Front Cardiovasc Med*. 2021;8:781393.
34. Kiss AR, Gregor Z, Popovics A, Grebur K, Szabó LE, Dohy Z, et al. Impact of Right Ventricular Trabeculation on Right Ventricular Function in Patients With Left Ventricular Non-compaction Phenotype. *Frontiers in Cardiovascular Medicine*. 2022;9.
35. Weir-McCall JR, Yeap PM, Papagiorcopulo C, Fitzgerald K, Gandy SJ, Lambert M, et al. Left Ventricular Noncompaction: Anatomical Phenotype or Distinct Cardiomyopathy? *J Am Coll Cardiol*. 2016;68(20):2157-65.
36. Captur G, Zemrak F, Muthurangu V, Petersen SE, Li C, Bassett P, et al. Fractal Analysis of Myocardial Trabeculations in 2547 Study Participants: Multi-Ethnic Study of Atherosclerosis. *Radiology*. 2015;277(3):707-15.
37. Gati S, Papadakis M, Papamichael ND, Zaidi A, Sheikh N, Reed M, et al. Reversible de novo left ventricular trabeculations in pregnant women: implications for the diagnosis of left ventricular noncompaction in low-risk populations. *Circulation*. 2014;130(6):475-83.
38. Gati S, Chandra N, Bennett RL, Reed M, Kervio G, Panoulas VF, et al. Increased left ventricular trabeculation in highly trained athletes: do we need more stringent criteria for the diagnosis of left ventricular non-compaction in athletes? *Heart*. 2013;99(6):401-8.
39. D'Ascenzi F, Pelliccia A, Natali BM, Bonifazi M, Mondillo S. Exercise-induced left-ventricular hypertrabeculation in athlete's heart. *Int J Cardiol*. 2015;181:320-2.
40. Adabifirouzjaei F, Igata S, DeMaria AN. Hypertrabeculation; a phenotype with Heterogeneous etiology. *Prog Cardiovasc Dis*. 2021;68:60-9.
41. Sedaghat-Hamedani F, Haas J, Zhu F, Geier C, Kayvanpour E, Liss M, et al. Clinical genetics and outcome of left ventricular non-compaction cardiomyopathy. *Eur Heart J*. 2017;38(46):3449-60.
42. Towbin JA, Lorts A, Jefferies JL. Left ventricular non-compaction cardiomyopathy. *Lancet*. 2015;386(9995):813-25.
43. Gruver EJ, Morgan JP, Stambler BS, Gwathmey JK. Uniformity of calcium channel number and isometric contraction in human right and left ventricular myocardium. *Basic Res Cardiol*. 1994;89(2):139-48.
44. Zemrak F, Ahlman MA, Captur G, Mohiddin SA, Kawel-Boehm N, Prince MR, et al. The relationship of left ventricular trabeculation to ventricular function and structure over a 9.5-year follow-up: the MESA study. *J Am Coll Cardiol*. 2014;64(19):1971-80.
45. Markovic NS, Dimkovic N, Damjanovic T, Loncar G, Dimkovic S. Isolated ventricular noncompaction in patients with chronic renal failure. *Clin Nephrol*. 2008;70(1):72-6.
46. Gati S, Papadakis M, Van Niekerk N, Reed M, Yeghen T, Sharma S. Increased left ventricular trabeculation in individuals with sickle cell anaemia: physiology or pathology? *Int J Cardiol*. 2013;168(2):1658-60.
47. Bleyl SB, Mumford BR, Thompson V, Carey JC, Pysher TJ, Chin TK, et al. Neonatal, lethal noncompaction of the left ventricular myocardium is allelic with Barth syndrome. *Am J Hum Genet*. 1997;61(4):868-72.

48. Kimura K, Takenaka K, Ebihara A, Uno K, Morita H, Nakajima T, et al. Prognostic impact of left ventricular noncompaction in patients with Duchenne/Becker muscular dystrophy--prospective multicenter cohort study. *Int J Cardiol.* 2013;168(3):1900-4.
49. Finsterer J, Stollberger C. Primary myopathies and the heart. *Scand Cardiovasc J.* 2008;42(1):9-24.
50. Piga A, Longo F, Musallam KM, Veltri A, Ferroni F, Chiribiri A, et al. Left ventricular noncompaction in patients with beta-thalassemia: uncovering a previously unrecognized abnormality. *Am J Hematol.* 2012;87(12):1079-83.
51. Stahli BE, Gebhard C, Biaggi P, Klaassen S, Valsangiacomo Buechel E, Attenhofer Jost CH, et al. Left ventricular non-compaction: prevalence in congenital heart disease. *Int J Cardiol.* 2013;167(6):2477-81.
52. Freedom RM, Yoo SJ, Perrin D, Taylor G, Petersen S, Anderson RH. The morphological spectrum of ventricular noncompaction. *Cardiol Young.* 2005;15(4):345-64.
53. Chung T, Yiannikas J, Lee LC, Lau GT, Kritharides L. Isolated noncompaction involving the left ventricular apex in adults. *Am J Cardiol.* 2004;94(9):1214-6.
54. Hanselmann A, Veltmann C, Bauersachs J, Berliner D. Dilated cardiomyopathies and non-compaction cardiomyopathy. *Herz.* 2020;45(3):212-20.
55. Arbustini E, Weidemann F, Hall JL. Left ventricular noncompaction: a distinct cardiomyopathy or a trait shared by different cardiac diseases? *J Am Coll Cardiol.* 2014;64(17):1840-50.
56. van Wanang JI, Caliskan K, Michels M, Schinkel AFL, Hirsch A, Dalinghaus M, et al. Cardiac Phenotypes, Genetics, and Risks in Familial Noncompaction Cardiomyopathy. *J Am Coll Cardiol.* 2019;73(13):1601-11.
57. Mazzarotto F, Hawley MH, Beltrami M, Beekman L, de Marvao A, McGurk KA, et al. Systematic large-scale assessment of the genetic architecture of left ventricular noncompaction reveals diverse etiologies. *Genet Med.* 2021;23(5):856-64.
58. Arbelo E, Protonotarios A, Gimeno JR, Arbustini E, Barriales-Villa R, Basso C, et al. 2023 ESC Guidelines for the management of cardiomyopathies. *Eur Heart J.* 2023.
59. Maron BJ, Towbin JA, Thiene G, Antzelevitch C, Corrado D, Arnett D, et al. Contemporary definitions and classification of the cardiomyopathies: an American Heart Association Scientific Statement from the Council on Clinical Cardiology, Heart Failure and Transplantation Committee; Quality of Care and Outcomes Research and Functional Genomics and Translational Biology Interdisciplinary Working Groups; and Council on Epidemiology and Prevention. *Circulation.* 2006;113(14):1807-16.
60. Aras D, Tufekcioglu O, Ergun K, Ozeke O, Yildiz A, Topaloglu S, et al. Clinical features of isolated ventricular noncompaction in adults long-term clinical course, echocardiographic properties, and predictors of left ventricular failure. *J Card Fail.* 2006;12(9):726-33.
61. Stanton C, Bruce C, Connolly H, Brady P, Syed I, Hodge D, et al. Isolated left ventricular noncompaction syndrome. *Am J Cardiol.* 2009;104(8):1135-8.
62. Oechslin EN, Attenhofer Jost CH, Rojas JR, Kaufmann PA, Jenni R. Long-term follow-up of 34 adults with isolated left ventricular noncompaction: a distinct cardiomyopathy with poor prognosis. *J Am Coll Cardiol.* 2000;36(2):493-500.
63. Petersen SE, Selvanayagam JB, Wiesmann F, Robson MD, Francis JM, Anderson RH, et al. Left ventricular non-compaction: insights from cardiovascular magnetic resonance imaging. *J Am Coll Cardiol.* 2005;46(1):101-5.

64. Grothoff M, Pachowsky M, Hoffmann J, Posch M, Klaassen S, Lehmkuhl L, et al. Value of cardiovascular MR in diagnosing left ventricular non-compaction cardiomyopathy and in discriminating between other cardiomyopathies. *Eur Radiol*. 2012;22(12):2699-709.
65. Stacey RB, Andersen MM, St Clair M, Hundley WG, Thohan V. Comparison of systolic and diastolic criteria for isolated LV noncompaction in CMR. *JACC Cardiovasc Imaging*. 2013;6(9):931-40.
66. Captur G, Muthurangu V, Cook C, Flett AS, Wilson R, Barison A, et al. Quantification of left ventricular trabeculae using fractal analysis. *J Cardiovasc Magn Reson*. 2013;15(1):36.
67. Vergani V, Lazzeroni D, Peretto G. Bridging the gap between hypertrabeculation phenotype, noncompaction phenotype and left ventricular noncompaction cardiomyopathy. *J Cardiovasc Med (Hagerstown)*. 2020;21(3):192-9.
68. Anderson RH, Jensen B, Mohun TJ, Petersen SE, Aung N, Zemrak F, et al. Key Questions Relating to Left Ventricular Noncompaction Cardiomyopathy: Is the Emperor Still Wearing Any Clothes? *Can J Cardiol*. 2017;33(6):747-57.
69. Grigoratos C, Barison A, Ivanov A, Andreini D, Amzulescu MS, Mazurkiewicz L, et al. Meta-Analysis of the Prognostic Role of Late Gadolinium Enhancement and Global Systolic Impairment in Left Ventricular Noncompaction. *JACC Cardiovasc Imaging*. 2019;12(11 Pt 1):2141-51.
70. Vaidya VR, Lyle M, Miranda WR, Farwati M, Isath A, Patlolla SH, et al. Long-Term Survival of Patients With Left Ventricular Noncompaction. *J Am Heart Assoc*. 2021;10(2):e015563.
71. Stampfli SF, Donati TG, Hellermann J, Anwer S, Erhart L, Gruner C, et al. Right ventricle and outcome in left ventricular non-compaction cardiomyopathy. *J Cardiol*. 2020;75(1):20-6.
72. Stampfli SF, Gotschy A, Kiarostami P, Ozkartal T, Gruner C, Niemann M, et al. Right ventricular involvement in left ventricular non-compaction cardiomyopathy. *Cardiol J*. 2020.
73. Arbustini E, Favalli V, Narula N, Serio A, Grasso M. Left Ventricular Noncompaction: A Distinct Genetic Cardiomyopathy? *J Am Coll Cardiol*. 2016;68(9):949-66.
74. Elliott P, Andersson B, Arbustini E, Bilinska Z, Cecchi F, Charron P, et al. Classification of the cardiomyopathies: a position statement from the European Society Of Cardiology Working Group on Myocardial and Pericardial Diseases. *Eur Heart J*. 2008;29(2):270-6.
75. Cavigli L, Focardi M, Cameli M, Mandoli GE, Mondillo S, D'Ascenzi F. The right ventricle in "Left-sided" cardiomyopathies: The dark side of the moon. *Trends Cardiovasc Med*. 2021;31(8):476-84.
76. Ponikowski P, Voors AA, Anker SD, Bueno H, Cleland JG, Coats AJ, et al. 2016 ESC Guidelines for the diagnosis and treatment of acute and chronic heart failure: The Task Force for the diagnosis and treatment of acute and chronic heart failure of the European Society of Cardiology (ESC). Developed with the special contribution of the Heart Failure Association (HFA) of the ESC. *Eur J Heart Fail*. 2016;18(8):891-975.
77. Oechslin E, Jenni R. Left ventricular non-compaction revisited: a distinct phenotype with genetic heterogeneity? *Eur Heart J*. 2011;32(12):1446-56.
78. Chin TK, Perloff JK, Williams RG, Jue K, Mohrmann R. Isolated noncompaction of left ventricular myocardium. A study of eight cases. *Circulation*. 1990;82(2):507-13.

79. Jenni R, Oechslin E, Schneider J, Attenhofer Jost C, Kaufmann PA. Echocardiographic and pathoanatomical characteristics of isolated left ventricular non-compaction: a step towards classification as a distinct cardiomyopathy. *Heart*. 2001;86(6):666-71.
80. Stollberger C, Finsterer J. Left ventricular hypertrabeculation/noncompaction. *J Am Soc Echocardiogr*. 2004;17(1):91-100.
81. Kohli SK, Pantazis AA, Shah JS, Adeyemi B, Jackson G, McKenna WJ, et al. Diagnosis of left-ventricular non-compaction in patients with left-ventricular systolic dysfunction: time for a reappraisal of diagnostic criteria? *Eur Heart J*. 2008;29(1):89-95.
82. Lindner JR. Contrast echocardiography: current status and future directions. *Heart*. 2021;107(1):18-24.
83. Bellavia D, Michelena HI, Martinez M, Pellikka PA, Bruce CJ, Connolly HM, et al. Speckle myocardial imaging modalities for early detection of myocardial impairment in isolated left ventricular non-compaction. *Heart*. 2010;96(6):440-7.
84. Peters F, Khandheria BK, Libhaber E, Maharaj N, Dos Santos C, Matioda H, et al. Left ventricular twist in left ventricular noncompaction. *Eur Heart J Cardiovasc Imaging*. 2014;15(1):48-55.
85. Arunamata A, Stringer J, Balasubramanian S, Tacy TA, Silverman NH, Punn R. Cardiac Segmental Strain Analysis in Pediatric Left Ventricular Noncompaction Cardiomyopathy. *J Am Soc Echocardiogr*. 2019;32(6):763-73 e1.
86. Dorobantu DM, Radulescu CR, Riding N, McClean G, de la Garza MS, Abuli-Lluch M, et al. The use of 2-D speckle tracking echocardiography in assessing adolescent athletes with left ventricular hypertrabeculation meeting the criteria for left ventricular non-compaction cardiomyopathy. *Int J Cardiol*. 2023;371:500-7.
87. Schulz-Menger J, Bluemke DA, Bremerich J, Flamm SD, Fogel MA, Friedrich MG, et al. Standardized image interpretation and post-processing in cardiovascular magnetic resonance - 2020 update : Society for Cardiovascular Magnetic Resonance (SCMR): Board of Trustees Task Force on Standardized Post-Processing. *J Cardiovasc Magn Reson*. 2020;22(1):19.
88. Csecs I, Czimbalmos C, Suhai FI, Mikle R, Mirzahosseini A, Dohy Z, et al. Left and right ventricular parameters corrected with threshold-based quantification method in a normal cohort analyzed by three independent observers with various training-degree. *Int J Cardiovasc Imaging*. 2018;34(7):1127-33.
89. Varga-Szemes A, Muscogiuri G, Schoepf UJ, Wichmann JL, Suranyi P, De Cecco CN, et al. Clinical feasibility of a myocardial signal intensity threshold-based semi-automated cardiac magnetic resonance segmentation method. *Eur Radiol*. 2016;26(5):1503-11.
90. Jaspers K, Freling HG, van Wijk K, Romijn EI, Greuter MJ, Willems TP. Improving the reproducibility of MR-derived left ventricular volume and function measurements with a semi-automatic threshold-based segmentation algorithm. *Int J Cardiovasc Imaging*. 2013;29(3):617-23.
91. Riffel JH, Schmucker K, Andre F, Ochs M, Hirschberg K, Schaub E, et al. Cardiovascular magnetic resonance of cardiac morphology and function: impact of different strategies of contour drawing and indexing. *Clin Res Cardiol*. 2019;108(4):411-29.
92. Amzulescu MS, De Craene M, Langet H, Pasquet A, Vancraeynest D, Pouleur AC, et al. Myocardial strain imaging: review of general principles, validation, and sources of discrepancies. *Eur Heart J Cardiovasc Imaging*. 2019;20(6):605-19.

93. Scatteia A, Baritussio A, Bucciarelli-Ducci C. Strain imaging using cardiac magnetic resonance. *Heart Fail Rev.* 2017;22(4):465-76.
94. van Dalen BM, Caliskan K, Soliman OI, Kauer F, van der Zwaan HB, Vletter WB, et al. Diagnostic value of rigid body rotation in noncompaction cardiomyopathy. *J Am Soc Echocardiogr.* 2011;24(5):548-55.
95. Notomi Y, Srinath G, Shiota T, Martin-Miklovic MG, Beachler L, Howell K, et al. Maturational and adaptive modulation of left ventricular torsional biomechanics: Doppler tissue imaging observation from infancy to adulthood. *Circulation.* 2006;113(21):2534-41.
96. Pua CJ, Loo G, Kui M, Moy WL, Hii AA, Lee V, et al. Impact of Diabetes on Myocardial Fibrosis in Patients With Hypertension: The REMODEL Study. *Circ Cardiovasc Imaging.* 2023;16(7):545-53.
97. Kawel-Boehm N, McClelland RL, Zemrak F, Captur G, Hundley WG, Liu CY, et al. Hypertrabeculated Left Ventricular Myocardium in Relationship to Myocardial Function and Fibrosis: The Multi-Ethnic Study of Atherosclerosis. *Radiology.* 2017;284(3):667-75.
98. Pelliccia A, Caselli S, Sharma S, Basso C, Bax JJ, Corrado D, et al. European Association of Preventive Cardiology (EAPC) and European Association of Cardiovascular Imaging (EACVI) joint position statement: recommendations for the indication and interpretation of cardiovascular imaging in the evaluation of the athlete's heart. *Eur Heart J.* 2018;39(21):1949-69.
99. Alfakih K, Plein S, Thiele H, Jones T, Ridgway JP, Sivananthan MU. Normal human left and right ventricular dimensions for MRI as assessed by turbo gradient echo and steady-state free precession imaging sequences. *J Magn Reson Imaging.* 2003;17(3):323-9.
100. Szucs A, Kiss AR, Suhai FI, Toth A, Gregor Z, Horvath M, et al. The effect of contrast agents on left ventricular parameters calculated by a threshold-based software module: does it truly matter? *Int J Cardiovasc Imaging.* 2019;35(9):1683-9.
101. Cerqueira MD, Weissman NJ, Dilsizian V, Jacobs AK, Kaul S, Laskey WK, et al. Standardized myocardial segmentation and nomenclature for tomographic imaging of the heart. A statement for healthcare professionals from the Cardiac Imaging Committee of the Council on Clinical Cardiology of the American Heart Association. *Circulation.* 2002;105(4):539-42.
102. Gregor Z, Kiss AR, Szabo LE, Toth A, Grebur K, Horvath M, et al. Sex- and age-specific normal values of left ventricular functional and myocardial mass parameters using threshold-based trabeculae quantification. *PLoS One.* 2021;16(10):e0258362.
103. Gregor Z, Kiss AR, Grebur K, Szabo LE, Merkely B, Vago H, et al. MR -specific characteristics of left ventricular noncompaction and dilated cardiomyopathy. *Int J Cardiol.* 2022;359:69-75.
104. Gregor Z, Kiss AR, Grebur K, Dohy Z, Kovacs A, Merkely B, et al. Characteristics of the right ventricle in left ventricular noncompaction with reduced ejection fraction in the light of dilated cardiomyopathy. *PLoS One.* 2023;18(9):e0290981.
105. Janik M, Cham MD, Ross MI, Wang Y, Codella N, Min JK, et al. Effects of papillary muscles and trabeculae on left ventricular quantification: increased impact of methodological variability in patients with left ventricular hypertrophy. *J Hypertens.* 2008;26(8):1677-85.

106. Czimbalmos C, Csecs I, Toth A, Kiss O, Suhai FI, Sydo N, et al. The demanding grey zone: Sport indices by cardiac magnetic resonance imaging differentiate hypertrophic cardiomyopathy from athlete's heart. *PLoS One*. 2019;14(2):e0211624.
107. Szucs A, Kiss AR, Gregor Z, Horvath M, Toth A, Dohy Z, et al. Changes in strain parameters at different deterioration levels of left ventricular function: A cardiac magnetic resonance feature-tracking study of patients with left ventricular noncompaction. *Int J Cardiol*. 2021;331:124-30.
108. Kawel-Boehm N, Maceira A, Valsangiacomo-Buechel ER, Vogel-Claussen J, Turkbey EB, Williams R, et al. Normal values for cardiovascular magnetic resonance in adults and children. *J Cardiovasc Magn Reson*. 2015;17:29.
109. Chung AK, Das SR, Leonard D, Peshock RM, Kazi F, Abdullah SM, et al. Women have higher left ventricular ejection fractions than men independent of differences in left ventricular volume: the Dallas Heart Study. *Circulation*. 2006;113(12):1597-604.
110. Natori S, Lai S, Finn JP, Gomes AS, Hundley WG, Jerosch-Herold M, et al. Cardiovascular function in multi-ethnic study of atherosclerosis: normal values by age, sex, and ethnicity. *AJR Am J Roentgenol*. 2006;186(6 Suppl 2):S357-65.
111. Petersen SE, Aung N, Sanghvi MM, Zemrak F, Fung K, Paiva JM, et al. Reference ranges for cardiac structure and function using cardiovascular magnetic resonance (CMR) in Caucasians from the UK Biobank population cohort. *J Cardiovasc Magn Reson*. 2017;19(1):18.
112. Le Ven F, Bibeau K, De Larocheiliere E, Tizon-Marcos H, Deneault-Bissonnette S, Pibarot P, et al. Cardiac morphology and function reference values derived from a large subset of healthy young Caucasian adults by magnetic resonance imaging. *Eur Heart J Cardiovasc Imaging*. 2016;17(9):981-90.
113. Le TT, Tan RS, De Deyn M, Goh EP, Han Y, Leong BR, et al. Cardiovascular magnetic resonance reference ranges for the heart and aorta in Chinese at 3T. *J Cardiovasc Magn Reson*. 2016;18:21.
114. Faganello G, Collia D, Furlotti S, Pagura L, Zaccari M, Pedrizzetti G, et al. A new integrated approach to cardiac mechanics: reference values for normal left ventricle. *Int J Cardiovasc Imaging*. 2020;36(11):2173-85.
115. Fiechter M, Fuchs TA, Gebhard C, Stehli J, Klaeser B, Stahli BE, et al. Age-related normal structural and functional ventricular values in cardiac function assessed by magnetic resonance. *BMC Med Imaging*. 2013;13:6.
116. Nikitin NP, Loh PH, de Silva R, Witte KK, Lukaschuk EI, Parker A, et al. Left ventricular morphology, global and longitudinal function in normal older individuals: a cardiac magnetic resonance study. *Int J Cardiol*. 2006;108(1):76-83.
117. Kaku K, Takeuchi M, Otani K, Sugeng L, Nakai H, Haruki N, et al. Age- and gender-dependency of left ventricular geometry assessed with real-time three-dimensional transthoracic echocardiography. *J Am Soc Echocardiogr*. 2011;24(5):541-7.
118. Ruan Q, Nagueh SF. Effect of age on left ventricular systolic function in humans: a study of systolic isovolumic acceleration rate. *Exp Physiol*. 2005;90(4):527-34.
119. Shub C, Klein AL, Zachariah PK, Bailey KR, Tajik AJ. Determination of left ventricular mass by echocardiography in a normal population: effect of age and sex in addition to body size. *Mayo Clin Proc*. 1994;69(3):205-11.
120. Yeon SB, Salton CJ, Gona P, Chuang ML, Blease SJ, Han Y, et al. Impact of age, sex, and indexation method on MR left ventricular reference values in the Framingham Heart Study offspring cohort. *J Magn Reson Imaging*. 2015;41(4):1038-45.

121. Cheng S, Fernandes VR, Bluemke DA, McClelland RL, Kronmal RA, Lima JA. Age-related left ventricular remodeling and associated risk for cardiovascular outcomes: the Multi-Ethnic Study of Atherosclerosis. *Circ Cardiovasc Imaging*. 2009;2(3):191-8.
122. Dannenberg AL, Levy D, Garrison RJ. Impact of age on echocardiographic left ventricular mass in a healthy population (the Framingham Study). *Am J Cardiol*. 1989;64(16):1066-8.
123. Kitzman DW, Scholz DG, Hagen PT, Ilstrup DM, Edwards WD. Age-related changes in normal human hearts during the first 10 decades of life. Part II (Maturity): A quantitative anatomic study of 765 specimens from subjects 20 to 99 years old. *Mayo Clin Proc*. 1988;63(2):137-46.
124. Olivetti G, Giordano G, Corradi D, Melissari M, Lagrasta C, Gambert SR, et al. Gender differences and aging: effects on the human heart. *J Am Coll Cardiol*. 1995;26(4):1068-79.
125. Kiss AR, Gregor Z, Furak A, Toth A, Horvath M, Szabo L, et al. Left ventricular characteristics of noncompaction phenotype patients with good ejection fraction measured with cardiac magnetic resonance. *Anatol J Cardiol*. 2021;25(8):565-71.
126. Kawamura T, Yasuda M, Okune M, Kakehi K, Kagioka Y, Nakamura T, et al. Increased Left Ventricular Trabeculation Is Associated With Increased B-Type Natriuretic Peptide Levels and Impaired Outcomes in Nonischemic Cardiomyopathy. *Can J Cardiol*. 2020;36(4):518-26.
127. Schuster A, Hor KN, Kowallick JT, Beerbaum P, Kutty S. Cardiovascular Magnetic Resonance Myocardial Feature Tracking: Concepts and Clinical Applications. *Circ Cardiovasc Imaging*. 2016;9(4):e004077.
128. Huttin O, Venner C, Frikha Z, Voilliot D, Marie PY, Aliot E, et al. Myocardial deformation pattern in left ventricular non-compaction: Comparison with dilated cardiomyopathy. *Int J Cardiol Heart Vasc*. 2014;5:9-14.
129. Niemann M, Liu D, Hu K, Cikes M, Beer M, Herrmann S, et al. Echocardiographic quantification of regional deformation helps to distinguish isolated left ventricular non-compaction from dilated cardiomyopathy. *Eur J Heart Fail*. 2012;14(2):155-61.
130. Cortes M, Oliva MR, Orejas M, Navas MA, Rabago RM, Martinez ME, et al. Usefulness of speckle myocardial imaging modalities for differential diagnosis of left ventricular non-compaction of the myocardium. *Int J Cardiol*. 2016;223:813-8.
131. Cheng H, Zhao S, Jiang S, Lu M, Yan C, Ling J, et al. Comparison of cardiac magnetic resonance imaging features of isolated left ventricular non-compaction in adults versus dilated cardiomyopathy in adults. *Clin Radiol*. 2011;66(9):853-60.
132. Donghi V, Tradi F, Carbone A, Viala M, Gaubert G, Nguyen K, et al. Left-ventricular non-compaction-comparison between different techniques of quantification of trabeculations: Should the diagnostic thresholds be modified? *Arch Cardiovasc Dis*. 2020;113(5):321-31.
133. Pan J, Wan Q, Li J, Wu H, Gao C, Tao Y, et al. Strain Values of Left Ventricular Segments Reduce Non-homogeneously in Dilated Cardiomyopathy with Moderately and Severely Deteriorated Heart Function Assessed by MRI Tissue Tracking Imaging. *Int Heart J*. 2018;59(6):1312-9.
134. Zheng T, Ma X, Li S, Ueda T, Wang Z, Lu A, et al. Value of Cardiac Magnetic Resonance Fractal Analysis Combined With Myocardial Strain in Discriminating Isolated Left Ventricular Noncompaction and Dilated Cardiomyopathy. *J Magn Reson Imaging*. 2019;50(1):153-63.

135. MacIver DH, Adeniran I, Zhang H. Left ventricular ejection fraction is determined by both global myocardial strain and wall thickness. *Int J Cardiol Heart Vasc.* 2015;7:113-8.
136. Gastl M, Gotschy A, Polacin M, Vishnevskiy V, Meyer D, Sokolska J, et al. Determinants of myocardial function characterized by CMR-derived strain parameters in left ventricular non-compaction cardiomyopathy. *Sci Rep.* 2019;9(1):15882.
137. Andre F, Steen H, Matheis P, Westkott M, Breuninger K, Sander Y, et al. Age- and gender-related normal left ventricular deformation assessed by cardiovascular magnetic resonance feature tracking. *J Cardiovasc Magn Reson.* 2015;17:25.
138. Stokke TM, Hasselberg NE, Smedsrud MK, Sarvari SI, Haugaa KH, Smiseth OA, et al. Geometry as a Confounder When Assessing Ventricular Systolic Function: Comparison Between Ejection Fraction and Strain. *J Am Coll Cardiol.* 2017;70(8):942-54.
139. Xu Y, He S, Li W, Wan K, Wang J, Mui D, et al. Quantitative mechanical dyssynchrony in dilated cardiomyopathy measured by deformable registration algorithm. *Eur Radiol.* 2020;30(4):2010-20.
140. Di Marco A, Anguera I, Schmitt M, Klem I, Neilan TG, White JA, et al. Late Gadolinium Enhancement and the Risk for Ventricular Arrhythmias or Sudden Death in Dilated Cardiomyopathy: Systematic Review and Meta-Analysis. *JACC Heart Fail.* 2017;5(1):28-38.
141. van Dalen BM, Caliskan K, Soliman OI, Nemes A, Vletter WB, Ten Cate FJ, et al. Left ventricular solid body rotation in non-compaction cardiomyopathy: a potential new objective and quantitative functional diagnostic criterion? *Eur J Heart Fail.* 2008;10(11):1088-93.
142. Maharaj N, Khandheria BK, Peters F, Libhaber E, Essop MR. Time to twist: marker of systolic dysfunction in Africans with hypertension. *Eur Heart J Cardiovasc Imaging.* 2013;14(4):358-65.
143. Nemes A, Foldeak D, Domsik P, Kalapos A, Sepp R, Borbenyi Z, et al. Different patterns of left ventricular rotational mechanics in cardiac amyloidosis-results from the three-dimensional speckle-tracking echocardiographic MAGYAR-Path Study. *Quant Imaging Med Surg.* 2015;5(6):853-7.
144. Jin SM, Noh CI, Bae EJ, Choi JY, Yun YS. Decreased left ventricular torsion and untwisting in children with dilated cardiomyopathy. *J Korean Med Sci.* 2007;22(4):633-40.
145. Setser RM, Kasper JM, Lieber ML, Starling RC, McCarthy PM, White RD. Persistent abnormal left ventricular systolic torsion in dilated cardiomyopathy after partial left ventriculectomy. *J Thorac Cardiovasc Surg.* 2003;126(1):48-55.
146. Popescu BA, Beladan CC, Calin A, Muraru D, Deleanu D, Rosca M, et al. Left ventricular remodelling and torsional dynamics in dilated cardiomyopathy: reversed apical rotation as a marker of disease severity. *Eur J Heart Fail.* 2009;11(10):945-51.
147. Ingels NB, Jr., Hansen DE, Daughters GT, 2nd, Stinson EB, Alderman EL, Miller DC. Relation between longitudinal, circumferential, and oblique shortening and torsional deformation in the left ventricle of the transplanted human heart. *Circ Res.* 1989;64(5):915-27.
148. Wulfsohn D, Nyengaard JR, Tang Y. Postnatal growth of cardiomyocytes in the left ventricle of the rat. *Anat Rec A Discov Mol Cell Evol Biol.* 2004;277(1):236-47.
149. Zheng T, Ma X, Li S, Ueda T, Wang Z, Lu A, et al. Value of Cardiac Magnetic Resonance Fractal Analysis Combined With Myocardial Strain in Discriminating Isolated

- Left Ventricular Noncompaction and Dilated Cardiomyopathy. *J Magn Reson Imaging*. 2019;50:156-63.
150. Oyama S, Sakuma M, Komaki K, Ishigaki H, Nakagawa M, Hozawa H, et al. Right ventricular systolic function and the manner of transformation of the right ventricle in patients with dilated cardiomyopathy. *Circ J*. 2004;68(10):933-7.
 151. Amzulescu MS, Rousseau MF, Ahn SA, Boileau L, de Meester de Ravenstein C, Vancraeynest D, et al. Prognostic Impact of Hypertrabeculation and Noncompaction Phenotype in Dilated Cardiomyopathy: A CMR Study. *JACC Cardiovasc Imaging*. 2015;8(8):934-46.
 152. Pueschner A, Chattranukulchai P, Heitner JF, Shah DJ, Hayes B, Rehwald W, et al. The Prevalence, Correlates, and Impact on Cardiac Mortality of Right Ventricular Dysfunction in Nonischemic Cardiomyopathy. *JACC Cardiovasc Imaging*. 2017;10(10 Pt B):1225-36.
 153. Stacey RB, Andersen M, Haag J, Hall ME, McLeod G, Upadhyya B, et al. Right ventricular morphology and systolic function in left ventricular noncompaction cardiomyopathy. *Am J Cardiol*. 2014;113(6):1018-23.
 154. Zhou X, Ferrara F, Contaldi C, Bossone E. Right Ventricular Size and Function in Chronic Heart Failure: Not to Be Forgotten. *Heart Fail Clin*. 2019;15(2):205-17.
 155. Leung SW, Elayi CS, Charnigo RJ, Jr., Syed MA. Clinical significance of right ventricular dysfunction in left ventricular non-compaction cardiomyopathy. *Int J Cardiovasc Imaging*. 2012;28(5):1123-31.
 156. Liu T, Gao Y, Wang H, Zhou Z, Wang R, Chang SS, et al. Association between right ventricular strain and outcomes in patients with dilated cardiomyopathy. *Heart* 2021;107(15):1233-9.
 157. Vijiic A, Onciul S, Guzu C, Verinceanu V, Bataila V, Deaconu S, et al. The prognostic value of right ventricular longitudinal strain and 3D ejection fraction in patients with dilated cardiomyopathy. *Int J Cardiovasc Imaging*. 2021;37(11):3233-44.
 158. Lisi M, Cameli M, Righini FM, Malandrino A, Tacchini D, Focardi M, et al. RV Longitudinal Deformation Correlates With Myocardial Fibrosis in Patients With End-Stage Heart Failure. *JACC Cardiovasc Imaging*. 2015;8(5):514-22.
 159. Gumus F, Durdu MS, Cakici M, Kurklu TST, Inan MB, Dincer I, et al. Right ventricular free wall longitudinal strain and stroke work index for predicting right heart failure after left ventricular assist device therapy. *Interact Cardiovasc Thorac Surg*. 2019;28(5):674-82.
 160. Alerhand S, Sundaram T, Gottlieb M. What are the echocardiographic findings of acute right ventricular strain that suggest pulmonary embolism? *Anaesth Crit Care Pain Med*. 2021;40(2):100852.
 161. Seo J, Jung IH, Park JH, Kim GS, Lee HY, Byun YS, et al. The prognostic value of 2D strain in assessment of the right ventricle in patients with dilated cardiomyopathy. *Eur Heart J Cardiovasc Imaging*. 2019;20(9):1043-50.
 162. Wang W, Chen W, Lin X, Fang L. Influence of Right Ventricular Dysfunction on Outcomes of Left Ventricular Non-compaction Cardiomyopathy. *Front Cardiovasc Med*. 2022;9:816404.
 163. Bucius P, Erley J, Tanacli R, Zieschang V, Giusca S, Korosoglou G, et al. Comparison of feature tracking, fast-SENC, and myocardial tagging for global and segmental left ventricular strain. *ESC Heart Fail*. 2020;7(2):523-32.

10. Bibliography of the candidate's publications

9.1. Publications related to dissertation

1. Gregor Z, Kiss AR, Szabo LE, Toth A, Grebur K, Horvath M, et al. Sex- and age-specific normal values of left ventricular functional and myocardial mass parameters using threshold-based trabeculae quantification. *PLoS One*. 2021;16(10):e0258362.
IF: 3.752
2. Gregor Z, Kiss AR, Grebur K, Szabo LE, Merkely B, Vago H, et al. MR -specific characteristics of left ventricular noncompaction and dilated cardiomyopathy. *Int J Cardiol*. 2022;359:69-75
IF: 3.5
3. Gregor Z, Kiss AR, Grebur K, Dohy Z, Kovacs A, Merkely B, et al. Characteristics of the right ventricle in left ventricular noncompaction with reduced ejection fraction in the light of dilated cardiomyopathy. *PLoS One*. 2023;18(9):e0290981.
IF: 3.7[#]

9.2. Publications not related to dissertation

1. Grebur K, Gregor Z, Kiss AR, Horvath M, Mester B, Czibalmos C, et al. Different methods, different results? Threshold-based versus conventional contouring techniques in clinical practice. *Int J Cardiol*. 2023;381:128-34.
IF: 3.5[#]
2. Juhasz V, Szabo L, Pavlik A, Tallay A, Balla D, Kiss O, et al. Short and mid-term characteristics of COVID-19 disease course in athletes: A high-volume, single-center study. *Scand J Med Sci Sports*. 2023;33(3):341-52.
IF: 4.1[#]
3. Babity M, Zamodics M, Konig A, Kiss AR, Horvath M, Gregor Z, et al. Cardiopulmonary examinations of athletes returning to high-intensity sport activity following SARS-CoV-2 infection. *Sci Rep*. 2022;12(1):21686.
IF: 4.6

4. Kiss AR, Gregor Z, Popovics A, Grebur K, Szabó LE, Dohy Z, et al. Impact of Right Ventricular Trabeculation on Right Ventricular Function in Patients With Left Ventricular Non-compaction Phenotype. *Frontiers in Cardiovascular Medicine*. 2022;9.
IF: 3.6
5. Lakatos BK, Tokodi M, Fabian A, Ladanyi Z, Vago H, Szabo L, et al. Frequent Constriction-Like Echocardiographic Findings in Elite Athletes Following Mild COVID-19: A Propensity Score-Matched Analysis. *Front Cardiovasc Med*. 2021;8:760651.
IF: 3.6
6. Kiss AR, Gregor Z, Furak A, Szabo LE, Dohy Z, Merkely B, et al. Age- and Sex-Specific Characteristics of Right Ventricular Compacted and Non-compacted Myocardium by Cardiac Magnetic Resonance. *Front Cardiovasc Med*. 2021;8:781393.
IF: 5.848
7. Kiss AR, Gregor Z, Furak A, Toth A, Horvath M, Szabo L, et al. Left ventricular characteristics of noncompaction phenotype patients with good ejection fraction measured with cardiac magnetic resonance. *Anatol J Cardiol*. 2021;25(8):565-71.
IF: 1.475
8. Szucs A, Kiss AR, Gregor Z, Horvath M, Toth A, Dohy Z, et al. Changes in strain parameters at different deterioration levels of left ventricular function: A cardiac magnetic resonance feature-tracking study of patients with left ventricular noncompaction. *Int J Cardiol*. 2021;331:124-30.
IF: 4.039
9. Szucs A*, Kiss AR*, Suhai FI, Toth A, Gregor Z, Horvath M, et al. The effect of contrast agents on left ventricular parameters calculated by a threshold-based software module: does it truly matter? *Int J Cardiovasc Imaging*. 2019;35(9):1683-9
IF: 1.969

*co-first authorship

#expected IF value

10. Acknowledgement

I would like to express my gratitude to all who made this PhD thesis possible.

I would like to thank Prof Dr Béla Merkely, the rector of Semmelweis University, for the years-long support as my tutor, and for the opportunity to carry out my research projects at the Heart and Vascular Center of Semmelweis University.

I would like to express my gratefulness to my tutor, Dr Andrea Szűcs, for her endless support, care and energy. Her personality and motivation inspired me since the beginning of my medical studies. I am more than thankful for her teaching and valuable advices in cardiology and also in personal life.

Special thanks to my colleague and friend-for-a-life, Dr Anna Réka Kiss, who motivated and supported me during the past years. She was always there for me in my clinical and private life, and her humor and attitude to life will always be exemplary for me. I am grateful for the countless joyful memories and unforgettable moments.

I would like to give special thanks to Dr Hajnalka Vágó for helping me with my research work. I am grateful for her valuable comments, advices and guidance.

I am thankful to Dr Attila Tóth his teaching in CMR evaluation processes and his help with statistical and IT questions any time needed.

I would like to thank Dr Márton Horváth, Dr Kinga Grebur, Dr Liliána Szabó, Dr Zsófia Dohy, Dr Csilla Czimbalmos, Dr Vencel Juhász, and all the student scientific researchers and radiology assistants for their help and support.

I would like to give special thanks to my family and friends for their encouragement and support in the past years. I am incredibly grateful to my husband, Péter Nagy, and my daughter Emma, for their patience and love in all situations, no matter how difficult they were.